

Protein Atlas. As shown in Table 2, there was no significant preference in the expression among the organs. Therefore, the

**Table 2. Identification of Chromosome X-Proteins in the Human Protein Atlas<sup>a</sup>**

	antibodies used	immunohistochemistry	
		strong (%)	weak (%)
Placenta	627	148 (23.6)	490 (78.1)
Kidney	900	149 (16.6)	654 (72.7)
Ovary	1180	160 (13.6)	825 (69.9)
Testis	1032	224 (21.7)	821 (79.6)
Brain	1112	159 (14.3)	776 (69.8)

<sup>a</sup>Placenta, kidney, ovary, testis and brain tissues were examined by immunohistochemistry using antibodies in the Human Protein Atlas (<http://www.proteinatlas.org/>). Numbers of antibodies used, stained the tissues strongly or more than weakly are shown (%).

Japan chromosome X project consortium preliminarily chose kidney, ovary, and breast as target sample tissues to look for chromosome X-proteins, which had not been well-identified yet because these organs had not been analyzed by other chromosome projects and our project members had already analyzed the proteomes of these organs more or less.

## 2. Collection of Protein Existence by MS

With informed consent, human kidney, ovary, breast tissues were obtained from patients when these organs or tissues were surgically removed for treatment of cancers. Kidneys were separated into cortex, medulla and glomerulus.<sup>8</sup> More fine structured (proximal tubule, distal tubule, collecting duct, and others) kidney sections were microdissected from kidney sections by laser microdissection system for deeper and more comprehensive MS analysis of kidney nephron parts. Other organs are also considered for such in depth MS analysis.

Members of the Japan Chromosome X Project are interested in MS analysis of cancers<sup>9–12</sup> and biofluids<sup>13,14</sup> for biomarker discovery and understanding of pathophysiology of cancers. Other members are also focusing on analysis of protein modification such as phosphorylation or glycosylation and collect MS evidence of post-translational modifications of chromosome X-proteins in the target organs and others.<sup>15</sup>

Another approach to find possible tissue or organ sites was carried out to develop a search engine (“Transcript Localizer”) to look at human microarray databases and to pick up sites where missing or unclear chromosome X genes are detected.

## 3. Collection of Protein Localization by Antibodies

Cellular localization of proteins, which would first be identified by MS in the target organs, was secondarily searched in the Human Protein Atlas database and the immunohistochemistry images were retrieved to combine to the data obtained by MS-based proteomics. A prototype of the human kidney proteome database has been opened to the public at the Web site of the HUPO Human Kidney and Urine Proteome Project (HKUPP) Initiative ([www.hkupp.org/](http://www.hkupp.org/)). The members of the chromosome X project also examined localization of MS-identified proteins in the target organs by immunohistochemistry to confirm the Human Protein Atlas data and the MS identification results. Our consortium will collect information on antibodies to the proteins, which are not provided by the Human Protein Atlas project, by searching in the Antibodypedia.

We are also developing an antibody search engine tool that looks for antibodies in open free access articles in the PubMed database and picks up antibodies to human proteins and collects the following information: name of companies providing antibodies and images obtained by the antibodies. Several different antibodies to one human protein were used in the past studies and the search engine collects information of all of these antibodies and will demonstrate antibody information in a rank order of number of articles in which the same antibody was used. This informs us which antibody is mostly used for a human protein in a community of scientists. Therefore, the tool was named “Antibody Ranker”. We believe this tool provides valuable information for researchers who are looking for antibodies for human proteins. Efficiency of the Antibody Ranker is also validated by selecting antibodies for immunohistochemistry in the chromosome X project.

## 4. Resources and Tools Developed from the Chromosome X Project

The Human Gene and Protein Database (HGPD; <http://www.HGPD.jp/>) launched in 2008 is a unique resource storing 43249 human Gateway entry clones constructed from the open reading frames (ORFs) of full-length human cDNA, which is the largest in the world.<sup>16</sup> Since the set of these clones are used for recombinant human protein synthesis by the wheat germ cell-free protein synthesis system, this resource is named the Human Proteome Expression Resource (HuPEX).<sup>17</sup> The recombinant protein resource has covered more than 85% of human proteins encoded by 20300 genes.

All synthesized proteins (approx. 18000) have been intensively analyzed by MS after trypsinization and MS/MS information of individual peptides from the proteins has been collected as a database for selection of peptides and MRM (multiple reaction monitoring) transitions. This provides us information to select peptides and MS/MS transitions for MRM (information-based MRM, iMRM) and also resources of reference peptides for quantitation of proteins in the target tissues.

## CONCLUSION

Current status and future plans of the Japan human chromosome X project are summarized in Figure 1 .. Collaboration and cooperation with other chromosome

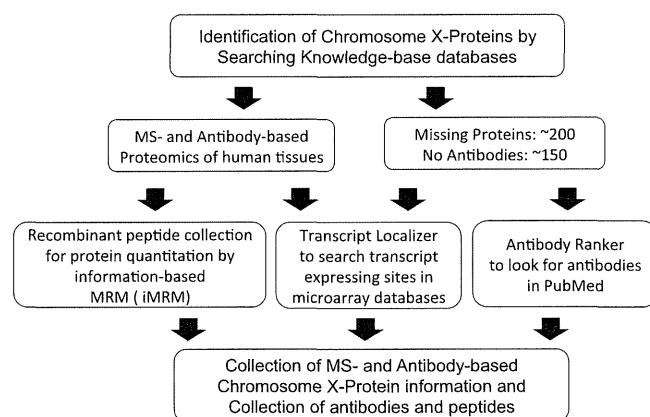


**Figure 1.** Workflow of Japan Chromosome X Project. Shown here is a strategy from basic collection of knowledge-base proteomics data to final completion of chromosome X proteome data and resource collection done by Japan Chromosome X Project Consortium.

projects in the Chromosome-centric Human Proteome Project, especially chromosome Y and with other Biology/Disease Human Proteome projects, need to be facilitated to complete the Human Proteome Project.

## AUTHOR INFORMATION

### Corresponding Author

\*E-mail: tdsymmt@med.niigata-u.ac.jp. Tel: +81-25-227-2151. Fax: +81-25-227-0768.

### Notes

The authors declare no competing financial interest.

## ACKNOWLEDGMENTS

This study was supported by a Grant-in-Aid for Scientific Research (B) to T.Y. ((21390262) from Japan Society for Promotion of Science and by a Grant-in-Aid for Strategic Research Project to T.Y. (500460) from Ministry of Education, Culture, Sports, Science and Technology, Japan and by a Grant-in-Aid for Diabetic Nephropathy and Nephrosclerosis Research from the Ministry of Health, Labor and Welfare of Japan.

## REFERENCES

- (1) Lane, L.; Argoud-Puy, G.; Britan, A.; Cusin, I.; Duek, P. D.; Evalet, O.; Gateau, A.; Gaudet, P.; Gleizes, A.; Masselot, A.; Zwahlen, C.; Bairoch, A. neXtProt: a knowledge platform for human proteins. *Nucleic Acids Res.* **2011**, *40*, D76–83.
- (2) Nguyen, D. K.; Disteche, C. M. High expression of the mammalian X chromosome in brain. *Brain Res.* **2006**, *1126*, 46–9.
- (3) Libert, C.; Dejager, L.; Pinheiro, I. The X chromosome in immune functions: when a chromosome makes the difference. *Nat. Rev. Immunol.* **2010**, *10*, 594–604.
- (4) Brockdorff, N. Chromosome silencing mechanisms in X-chromosome inactivation: unknown unknowns. *Development* **2011**, *138*, 5057–65.
- (5) Reinius, B.; Shi, C.; Hengshuo, L.; Sandhu, K. S.; Radomska, K. J.; et al. Female-biased expression of long non-coding RNAs in domains that escape X-inactivation in mouse. *BMC Genomics* **2010**, *11*, 614.
- (6) Uhlen, M.; Oksvold, P.; Fagerberg, L.; Lundberg, E.; Jonasson, K.; Forsberg, M.; Zwahlen, M.; Kampf, C.; Wester, K.; Hober, S.; Wernerus, H.; Björling, L.; Ponten, F. Towards a knowledge-based Human Protein Atlas. *Nat. Biotechnol.* **2010**, *28*, 1248–50.
- (7) Ross, M.; Grafham, D. V.; Coffey, A. J.; Scherer, S.; McLay, K.; et al. The DNA sequence of the human X chromosome. *Nature* **2005**, *434*, 325–37.
- (8) Miyamoto, M.; Yoshida, Y.; Taguchi, I.; Nagasaka, Y.; Tasaki, M.; et al. In-depth proteomic profiling of the normal human kidney glomerulus using two-dimensional protein prefractionation in combination with liquid chromatography-tandem mass spectrometry. *J Proteome Res.* **2007**, *6*, 3680–90.
- (9) Masuishi, Y.; Arakawa, N.; Kawasaki, H.; Miyagi, E.; Hirahara, F.; Hirano, H. Wild-type p53 enhances annexin IV gene expression in ovarian clear cell adenocarcinoma. *FEBS J.* **2011**, *27*, 1470–83.
- (10) Muraoka, S.; Kume, H.; Watanabe, S.; Adachi, J.; Kuwano, M.; et al. Strategy for SRM-based verification of biomarker candidates discovered by iTRAQ method in limited breast cancer tissue samples. *J. Proteome Res.* **2012**, *11*, 4201–10.
- (11) Ono, M.; Kamita, M.; Murakoshi, Y.; Matsubara, J.; Honda, K.; et al. Biomarker discovery of pancreatic and gastrointestinal cancer by 2DICAL: 2-dimensional image-converted analysis of liquid chromatography and mass spectrometry. *Int. J. Proteomics.* **2012**, *2012*, 897412.
- (12) Sugihara, Y.; Taniguchi, H.; Kushima, R.; Tsuda, H.; Kubota, D.; et al. Proteomic-based identification of the APC-binding protein EB1 as a candidate of novel tissue biomarker and therapeutic target for colorectal cancer. *J. Proteomics* **2012**, *75*, 5342–55.
- (13) Kawashima, Y.; Fukutomi, T.; Tomonaga, T.; Takahashi, H.; Nomura, F.; Maeda, T.; Kodera, Y. High-yield peptide-extraction method for the discovery of subnanomolar biomarkers from small serum samples. *J. Proteome Res.* **2010**, *9*, 1694–705.
- (14) Kobayashi, M.; Matsumoto, T.; Ryuge, S.; Yanagita, K.; Nagashio, R.; et al. CAXII Is a sero-diagnostic marker for lung cancer. *PLoS One* **2012**, *7*, e33952.
- (15) Imamura, H.; Wakabayashi, M.; Ishihama, Y. Analytical strategies for shotgun phosphoproteomics: status and prospects. *Semin. Cell Dev. Biol.* **2012**, *23*, 836–42.
- (16) Goshima, N.; Kawamura, Y.; Fukumoto, A.; Miura, A.; Honma, R.; et al. Human protein factory for converting the transcriptome into an in vitro-expressed proteome. *Nat. Methods* **2008**, *5*, 1011–7.
- (17) Maruyama, Y.; Kawamura, Y.; Nishikawa, T.; Isogai, T.; Nomura, N.; Goshima, N. HGPS: Human Gene and Protein Database, 2012 update. *Nucleic Acids Res.* **2012**, *40*, D924–9.

# Identification of Phosphorylated Proteins Involved in the Oncogenesis of Prostate Cancer Via Pin1-Proteomic Analysis

Kanji Endoh,<sup>1,2</sup> Mayuko Nishi,<sup>2</sup> Hitoshi Ishiguro,<sup>3,4</sup> Hiroji Uemura,<sup>3</sup> Yohei Miyagi,<sup>5</sup> Ichiro Aoki,<sup>6</sup> Hisashi Hirano,<sup>7</sup> Yoshinobu Kubota,<sup>3</sup> and Akihide Ryo<sup>2\*</sup>

<sup>1</sup>Drug Discovery Research Center, Taiho Pharmaceutical Co., Ltd, Tsukuba, Japan

<sup>2</sup>Department of Microbiology, Yokohama City University School of Medicine, Yokohama, Japan

<sup>3</sup>Department of Urology, Yokohama City University School of Medicine, Yokohama, Japan

<sup>4</sup>Photocatalyst Group, Kanagawa Academy of Science and Technology, Takatsu-ku, Kawasaki, Kanagawa, Japan

<sup>5</sup>Molecular Pathology and Genetics Division, Kanagawa Cancer Center Research Institute, Yokohama, Japan

<sup>6</sup>Department of Molecular Pathology, Yokohama City University School of Medicine, Yokohama, Japan

<sup>7</sup>Department of Nanobioscience, Yokohama City University, Yokohama, Japan

**BACKGROUND.** The peptidyl-prolyl isomerase Pin1 regulates a subset of phosphorylated proteins by catalyzing the *cis-trans* isomerization of their specific phosphorylated Ser/Thr-Pro motifs. Although Pin1 has been shown to be involved in cell transformation and the maintenance of the malignant phenotype in prostate cancer, its specific substrates during these processes have not yet been determined.

**METHODS.** Cancer-specific phosphorylated proteins were isolated from two human prostate cancer cell lines (PC-3, LNCaP) and the Dunning rat prostate cancer cell lines by GST-pull down analysis with recombinant GST-Pin1 protein. These proteins were then identified by the LC-MS/MS analysis using a Q-ToF micro mass spectrometer and processed for further functional analysis.

**RESULTS.** We newly identified five prostate cancer-specific Pin1 binding proteins (PINBPs) in this screen. Among these, TRK-fused gene (TFG) was found to be preferentially up-regulated in prostate cancer cell lines and tissues. The targeted inhibition of TFG by specific siRNA resulted in the reduced cell proliferation and the induction of premature senescence in PC3 prostate cancer cells. We further found that TFG can facilitate the cell signaling mediated by NF-kappaB and androgen receptor (AR). Tissue micro-dissection based quantitative RT-PCR analysis of prostate cancer tissues following radical prostatectomy further revealed that TFG expression is closely associated with both a higher probability and shorter period of tumor recurrence following surgery.

**CONCLUSIONS.** Pin1-based proteomics analysis is a useful tool for the identification of prostate cancer-specific phosphorylated proteins. TFG could be a potential diagnostic and/or prognostic marker and therapeutic target in prostate cancer. *Prostate* 72:626–637, 2012. © 2011 Wiley Periodicals, Inc.

**KEY WORDS:** prostate cancer; tumor recurrence; androgen receptor; prognostic marker

## INTRODUCTION

Prostate cancer is one of the most common tumors to arise in males and its incidence is increasing steadily worldwide [1]. Despite the possibility of an earlier diagnosis using serum prostate specific antigen (PSA), prostate cancer is still the leading cause of male cancer death in many countries [2]. Radiation and a radical prostatectomy are definitive forms of therapy for clinically localized prostate cancers, but a

Grant sponsor: Special Coordination Funds for Promoting Science and Technology; Grant sponsor: Takeda Foundation; Grant sponsor: Uehara Memorial Foundation; Grant sponsor: Grant-in-Aid for Scientific Research on Innovative Areas.

\*Correspondence to: Prof. Akihide Ryo, PhD, MD, Yokohama City University School of Medicine, 3-9 Fukuura, Kanazawa-ku, Yokohama 236-0004, Japan. E-mail: aryo@yokohama-cu.ac.jp

Received 21 March 2011; Accepted 1 July 2011

DOI 10.1002/pros.21466

Published online 1 August 2011 in Wiley Online Library (wileyonlinelibrary.com).

substantial number of cases have demonstrated tumor recurrence, even when tumors have been localized pathologically to the prostate at the time of surgery. Recurrent cancers after radiation and radical prostatectomy are often refractory to treatments with chemical reagents and radiation [3,4]. Although the Gleason grade is an excellent diagnostic indicator of prostate cancer based on histopathological features, it is currently difficult to predict whether a clinically localized prostate cancer will remain latent or progress to aggressive or metastatic disease [5]. Novel prostate cancer biomarkers based on the molecular cell biology of prostate tumorigenesis are thus desirable.

Recent advances in mass spectrometry (MS) have enabled the analysis of not only overall protein expression profiling in certain cancer cells or tissues [6–8], but also a substantial number of post-translational modifications (PTMs), such as protein phosphorylation, from small cancer tissue specimens in a short timeframe. Whilst these technically advanced MS methods can detect a large number of candidate proteins [9,10], it remains difficult to select functionally significant oncoproteins and the corresponding PTMs that contribute to the progression of cellular oncogenesis. It is thus desirable to develop a new strategy for selectively capturing phosphorylated proteins that are functionally important in cell transformation and oncogenesis.

Pin1 is an enzyme that specifically binds phosphorylated serine or threonine, immediately preceding proline (pSer/Thr-Pro) in a subset of proteins [11]. Pin1 regulates the function of its substrate proteins by promoting *cis/trans* isomerization of the peptide bond between Ser/Thr and Pro [12,13]. We previously demonstrated that the peptidyl prolyl-isomerase Pin1 plays an important role in the maintenance of the tumorigenic properties of prostate cancer [14]. Targeted depletion of Pin1 results in the stable suppression of both cell growth and tumorigenicity in prostate cancer cells [14]. Furthermore, Pin1 inhibition significantly suppresses several malignant phenotypes such as cell proliferation, invasion, and angiogenesis. These results indicate that Pin1 plays crucial role in a range of tumorigenic properties in prostate cancer cells. However, specific Pin1 substrates during these processes have not so far been determined.

In our present study, we utilized Pin1 as a molecular probe in combination with MS analysis to capture and identify prostate cancer-specific phosphorylated proteins. We thereby identified TRK-fused gene (TFG) as a new Pin1-interacting oncogenic protein and provide evidence that it could be a potent therapeutic target for prostate cancer.

## MATERIALS AND METHODS

### Cell Lines

DU145, PC3, and LNCaP cells (human prostate cancer cell lines) were obtained from the American Type Culture Collection (Rockville, MD). Prostatic epithelial cells (hPrEC) were purchased from Takara Bio (Shiga, Japan). PrEC were cultured in prostate epithelial basal medium (PrEBM, Takara Bio) supplemented with human epidermal growth factor, triiodothyronine, transferrin, epinephrine, gentamicin sulfate, amphotericin B, bovine pituitary extract, bovine insulin, hydrocortisone, and retinoic acid additives provided by the manufacturer. Prior to the experiments, DU145, LNCaP, and PC3 cells were cultured in RPMI1640 (Wako, Osaka, Japan) supplemented with 10% fetal calf serum (FCS), and incubated under 5% CO<sub>2</sub>. In the experiments, these cells were cultured in phenol red-free RPMI plus 0.1% bovine serum albumin (BSA) or F-12 medium supplemented with charcoal-stripped 10% FCS, and stimulated with reagents.

### Pin1 Proteomic Analysis

GST-fused Pin1 was purified using a conventional strategy in *E. Coli* and used in pull down analysis with cell lysates. Prostate cancer or normal prostate epithelial cell lysates were processed for pull down with GST or GST-Pin1 at 4°C for 3 hr. Pin1-binding proteins were thereby recovered and collected by thrombin cleavage which digests at a site between GST and Pin1 followed by SDS-PAGE, as described previously [15]. Gels were subjected to silver staining and specific bands were systematically excised. The gel pieces were then reduced, alkylated, and trypsinized. Peptides were analyzed by liquid chromatography-tandem MS (LC-MS/MS) analysis with a Q-ToF micro Mass Spectrometer (Micromass). Protein identification was performed using a Mascot search (Matrix Science).

### RNA Extraction, cDNA Preparation, Real-Time RT-PCR, and siRNA

Total RNA was extracted using ISOGEN reagent (Nippon Gene, Tokyo, Japan). Quantitative reverse transcription (qRT)-PCR was performed with an ABI 7700 sequence detector system (Applied Biosystems) as described previously. Primers for TFG (5'-GGAA-CACAAAAGACCAAAATGG-3'; 5'-AGGGCTCTAC-TTTAGTACATC-3) were designed using Primer Express (Applied Biosystems). Reagents from the One-Step Cyber Green RT-PCR Master Mix Reagents Kit (TaKaRa) were used in accordance with the

manufacturer's protocol. PCR reactions were performed in a total volume of 25  $\mu$ l using ABI Prism770 (Applied Biosystems). A standard curve method was used to determine the expression levels and all measurements were found to be within the linear range of the standard curve.  $\beta$ -actin was used as an internal control and to normalize Pin1 expression levels. TFG-targeted siRNA sequences were as follows: (TFG1: 5'-GUCUGCUUCUGAUUCUUCU-3'; TFG2: 5'-GGU-CAGAUGUACCAACAGU-3'; control: 5'-UCGTAU-GUUGUGUGGAAU-3').

### Cell Culture

Human prostate cancer cell lines PC3, LNCaP, and DU145 were cultured in RPMI1640 or DMEM, supplemented with 10% FCS and penicillin/streptomycin. Dunning rat tumor sub lines of variable cell growth (doubling time, days) and variable degrees of metastatic potential; AT-1 ( $2.5 \pm 0.2$  days, 0–5%), AT-2 ( $2.5 \pm 0.2$  days, 0–20%), AT-3 ( $1.8 \pm 0.2$  days, 75–100%), and MAT-LyLu ( $1.7 \pm 0.3$  days, 75–100%) were grown in RPMI 1,640/10% fetal bovine serum (FBS) supplemented with 0.1% dexamethasone and 1% L-glutamine [16].

### Antibodies

An anti-TFG polyclonal antibody was generated in rabbits against a synthetic peptide corresponding to the region 320–336 of TFG conjugated to keyhole limpet hemocyanin, and purified on a peptide affinity column. TFG phospho-specific polyclonal antibodies (anti-TFGpThr206 and anti-TFGpThr372) were generated in rabbits against synthetic peptides "CEDRSGpTPDSIX" and "CXXGSTMpTPPPSX" (where X donates any one of the 20 amino acids) respectively, as described previously [17]. Antibodies were affinity-purified on sepharose resin to which the appropriate phosphorylated peptide had been covalently coupled and passed through a column containing the unphosphorylated peptides to remove any antibodies that did not recognize the phosphorylated epitope. Phosphospecificity was established by ELISA and western blot assays.

### Gene Reporter Assay

Cells were transfected with plasmid vectors encoding either NF- $\kappa$ B-Luc or PSA-Luc reporter construct and co-transfected with pRL-TK or pRL-SV40 using Effectene transfection reagent (Qiagen). One day after transfection, the cells were resuspended in passive lysis buffer (Promega) and incubated for 15 min at room temperature. Luciferase activities were measured with a Dual-Luciferase reporter assay

system (Promega) according to the manufacturer's instructions.

### Patients and Samples

Paired human untreated primary prostate cancer tissues and normal (or benign prostatic hypertrophy (BPH) ( $n = 29$ )) tissues from same patients were obtained during radical prostatectomy at Yokohama City University Hospital and its affiliates. The clinicopathological data for these samples are summarized in Table I. The postoperative serum PSA levels were assayed every 2–3 months. The occurrence of these consecutive elevations of the PSA level by more than 0.20 ng/ml was defined as biochemical recurrence [18]. The pathological stage was determined according to the International Union against Cancer (UICC) [19]. The sampling and usage of all prostate tissues in this study were approved by the ethical committee of Yokohama City University Graduate School of Medicine and performed only after obtaining informed consent from each patient.

### Statistics

All statistical analyses were performed using a software for statistic analysis PASW statistics 18 (SPSS, Chicago, IL). TFG expressions and clinicopathological characteristics were compared using chi-square test or the Fisher's exact test. For analysis of the correlation between TFG expression, clinicopathological characteristics, and biochemical recurrence, Kaplan–Meier and log rank tests were utilized. Each parameter and biochemical recurrence was further analyzed using a Cox promotional hazard regression model in univariate and multivariate analyses. The hazard ratio and 95% confidence interval (95%) are also shown in the results.  $P \leq 0.05$  was considered to be statistically significant.

**TABLE I. Clinicopathological Characteristics of Examined Prostate Cancer Samples**

		n	(%)
Age (years)	$\leq 68$	15	51.7
	$>68$	14	48.3
Median(Range) Preoperative PSA(ng/ml)	$\leq 10.0$	15	51.7
	$>10.0$	14	48.3
Median(Range) UICC Stage	8.8(4.1–35.7)		
Gleason score	pT2a-b	16	55.2
	pT3a-b	13	44.8
	$\leq 7$	20	69.0
	$>8$	9	31.0

**RESULTS**

**Isolation of Prostate Cancer-Specific Phosphorylated Proteins using Pin1 Proteomics**

Previous reports of Pin1-prostate cancer interaction have demonstrated that Pin1 contributes to the transformation and tumorigenicity of prostate epithelial cells by modulating the function of its substrate proteins [20]. To identify prostate cancer-specific Pin1 substrates, we performed proteomics analysis in which Pin1 was used as a molecular probe to detect phosphorylated targets. We detected multiple bands in then prostate cancer cell lines that were not present in normal prostate epithelial cells. These bands were excised from the gel and subjected to in-gel digestion followed by LC-MS/MS analysis with a Micromass Q-ToF micro Mass Spectrometer. We identified five Pin1 binding proteins (PINBP 1-5) specific to prostate cancer cells (Fig. 1, left panel).

We next performed parallel experiments using the Dunning rat tumor model developed by Issacs et al. [16]. This is a well-characterized animal model that has been used to study prostate cancer pathogenesis. These cell lines have also been shown to exhibit many characteristics including the androgen responsiveness and differential metastatic ability observed during the progression of human prostate cancer. We investigated Pin1-binding proteins in several Dunning tumor sublines (AT1, AT-2, AT-3, and MAT-LyLu), the spectra of which are illustrated in Figure 1 (right panel). When we evaluated the differences in the PINBP profiles for each subline, a 55 kDa band was found to be prominent. This band intensity was significantly increased in malignant Dunning tumor cells. Subsequent LS-MS/MS analysis revealed that the corresponding protein is derived from rat TFG. Since TFG was also identified as a Pin1-interacting protein in human prostate cancer cell lines, we focused on this protein for further analysis.

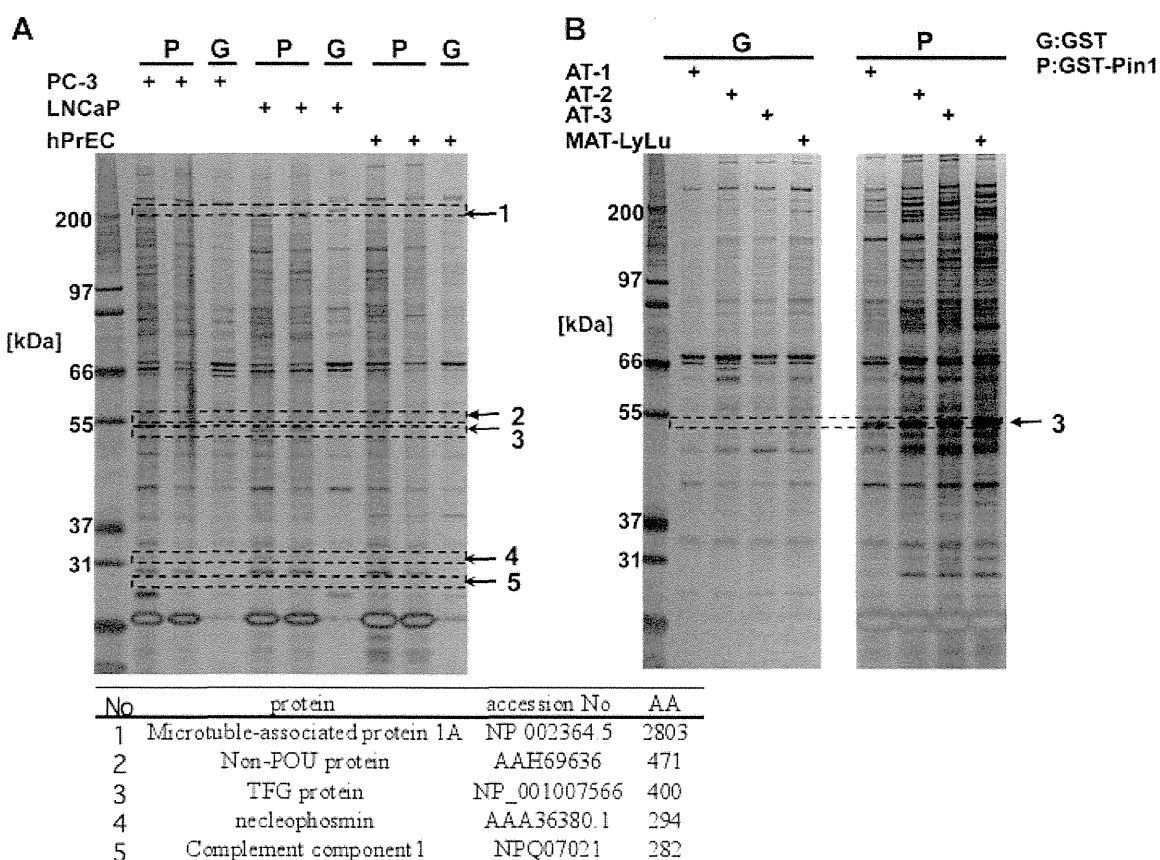


**Fig. 1.** Identification of TFG as a Pin1 binding protein in prostate cancer cells. **A:** Cell lysates of PC-3, LNCaP, or normal prostatic epithelial cells (hPrEC) were subjected to pull down analysis with either GST or GST-Pin1. Proteins bound to glutathione sepharose beads were isolated and detected by SDS-PAGE and silver staining. Arrows point to the bands containing TFG protein. **B:** Cell lysates from each Dunning subline were processed for GST-pull down analysis as in (A). Bound proteins were separated by SDS-PAGE and detected by silver staining. Arrow indicates the bands containing TFG protein.

### TFG is Overexpressed in Prostate Cancer Cells and Tissues

Our initial analysis indicated that TFG is a Pin1-binding protein in prostate cancer cells and we thus examined its expression in these cells. Both quantitative RT-PCR analysis and immunoblotting with TFG antibodies revealed that TFG expression is preferentially up-regulated in prostate cancer cell lines as compared with normal prostate epithelial cells (Fig. 2A and B). Immunohistochemical analysis of representative prostate cancer tissues with TFG antibodies further revealed that TFG is expressed in glandular cancer cells but not in adjacent non-cancerous epithelial cells (benign prostatic hyperplasia: BPH) or interstitial cells (Fig. 2C). Since prostate cancer cells often infiltrate non-cancerous glands and the intervening fibro-muscular stroma, it was necessary to precisely quantitate the TFG expression levels in cancerous glandular cells. We utilized tissue microdissection based quantitative RT-PCR analysis for this

purpose. Twenty nine paired human prostate cancer and adjacent non-cancerous prostate tissues from the same individual were thereby examined. The results of this analysis showed that the TFG expression levels in prostate cancer tissues are higher than in non-cancerous tissues in 63.9% ( $P = 0.031$ ) of the cases (Fig. 2D). These results together demonstrate that TFG is overexpressed in prostate cancer cells.

### TFG Interacts With Pin1 on its Thr206-Pro and Thr372-Pro Motifs

Previous reports have indicated that Pin1 can bind only phosphorylated Ser/Thr-Pro motifs [21] of which only two (Thr206-Pro and Thr372-Pro) are present in the TFG protein (Fig. 3A, upper). Interestingly, this motif is conserved between various species including human, rhesus monkey, mouse, and xenopus (Fig. 3A, lower). We thus generated TFG site-directed mutants at these sites by substituting threonine with alanine (T206A, T372A). GST-pull down

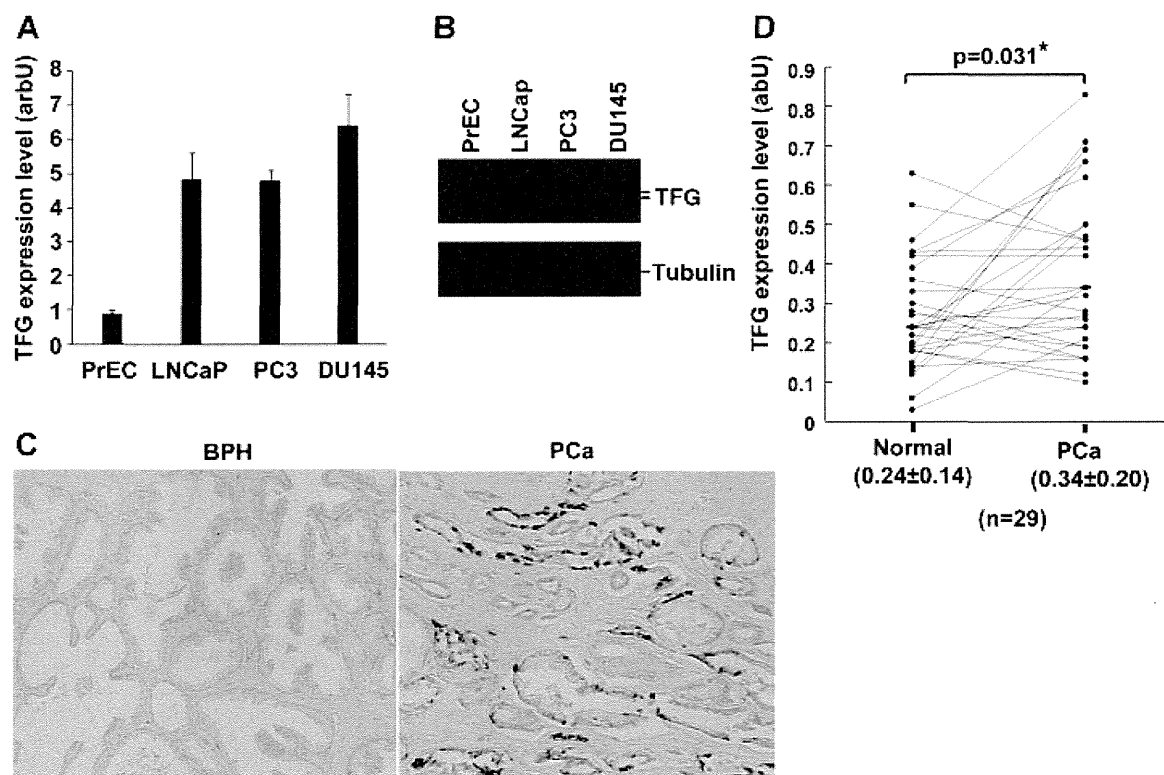


**Fig. 2.** TFG is overexpressed in prostate cancer cells and tissues. **A, B:** TFG mRNA expression levels were monitored by quantitative RT-PCR analysis of normal prostatic epithelial cells (PrEC) or three different prostate cancer cell lines (A). Cell lysates from the indicated cells were subjected to immunoblot analysis with either anti-TFG or anti-tubulin antibody. Tubulin was used as a loading control. **C:** Immunostaining of TFG in human prostate cancer. Sections from paraffin-embedded tissues were subjected to antigen retrieval, followed by immunostaining with anti-TFG antibody. Non-cancerous benign epithelial hyperplastic tissues (left) show no visually detectable TFG staining, while invasive prostate cancer cells (right) show focally, but intense TFG staining. **D:** TFG mRNA expression levels in prostate cancer tissues and adjacent normal tissues ( $n = 29$ ). TFG expression in prostate cancer was significantly higher than that in normal prostate tissue (Mann-Whitney U-test,  $P = 0.031$ ,  $^*P < 0.05$ ).

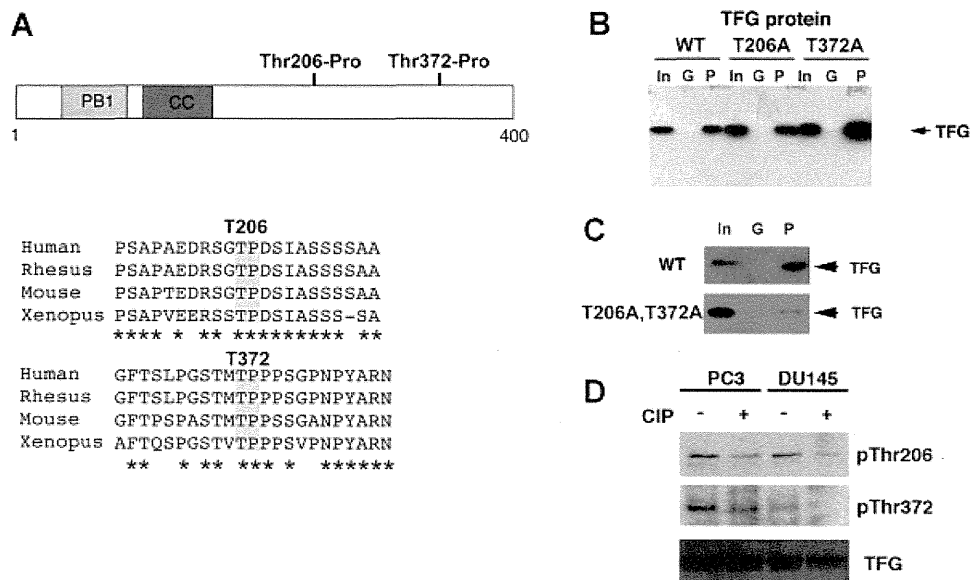


**Fig. 3.** TFG interacts with Pin1 via its Thr206-Pro and Thr372-Pro motifs. **A:** Schematic representation of human TFG protein (upper). Amino acid sequence alignment of the human, rhesus, mouse, and xenopus TFG proteins (lower). The conserved Thr206-Pro and Thr372 motifs are boxed. **B:** PC3 cells were transfected with the FLAG-tagged TFG (wild-type, WT) or its site-directed mutants, TFG-T206A, or TFG-T372A. At 24 hr following transfection, cell lysates were subjected to GST pull-down analysis followed by immunoblotting with anti-FLAG antibody. In, Input; G, GST; P, GST-Pin1. **C:** PC3 cells were transfected with either FLAG-tagged TFG (wild-type, WT) or its site-directed mutant on both Thr206 and Thr372 sites (T206, 372A). At 24 hr following transfection, cell lysates were subjected to GST pull-down analysis followed by immunoblotting with anti-FLAG antibody. **D:** Lysates from PC3 or DU145 cells were treated or untreated with calf-intestine alkaline phosphatase (CIP) followed by immunoblotting analysis with an anti-TFG antibody or phospho-specific antibodies targeting p-Thr206 or p-Thr372, respectively.

analysis subsequently revealed that Pin1 binds wild-type TFG and its single site-directed mutants (T206A, T372A) (Fig. 3B), but fails to interact with the corresponding TFG double mutant (2A: T206A, T372A) (Fig. 3C). These results indicate that Pin1 binds TFG on both the Thr206-Pro and Thr372-Pro motifs.

We next addressed whether Pin1 binding sites in TFG were indeed phosphorylated in prostate cancer cells. Cell lysates from PC3 and DU145 cells were treated or untreated with calf-intestine alkaline phosphatase and then subjected to immunoblotting analysis with Thr206 or Thr372 phospho-specific antibodies. We found that these two sites are indeed phosphorylated in the two prostate cancer cell lines as the signals were abolished by the pre-treatment with alkaline phosphatase (Fig. 3D). These results together indicate that Pin1 interacts with the phosphorylated Thr206 and Thr372 sites on TFG.

#### TFG Activates NF-kappaB in Cooperation With Pin1

A previous report has indicated that TFG binds NEMO and TANK proteins that modulate the NF-kappaB pathway and enhance NF-kappaB activity [21]. We thus speculated as to whether Pin1 enhances

the function of TFG during NF-kappaB signaling. A luciferase reporter assay using the 3X kappaB-luciferase reporter construct was performed in LNCaP cells co-transfected with TFG or Pin1. Whilst the sole expression of either TFG or Pin1 had only minor effects, the co-expression of TFG and Pin1, but not its catalytic domain mutant (K63A), produced a significant increase in reporter activity (Fig. 4A). However, this is not the case in the TFG mutant lacking two Pin1 binding sites (T206A, T372A; Fig. 4B). This indicated that Pin1 promotes TFG-mediated NF-kappaB activation via its interaction with the Thr206-Pro and Thr372-Pro motifs on TFG.

#### TFG Promotes the Transcriptional Activity of AR

We next tested whether Pin1 enhances the transcriptional activity of androgen receptor (AR). A luciferase reporter assay using a PSA promoter containing androgen responsive elements (AREs) was performed in either LNCaP or 293T cells co-transfected with AR or TFG. Whilst the sole expression of TFG had no significant effects, the co-expression of TFG and AR produced a significant increase in the reporter activity of the PSA promoter with and without



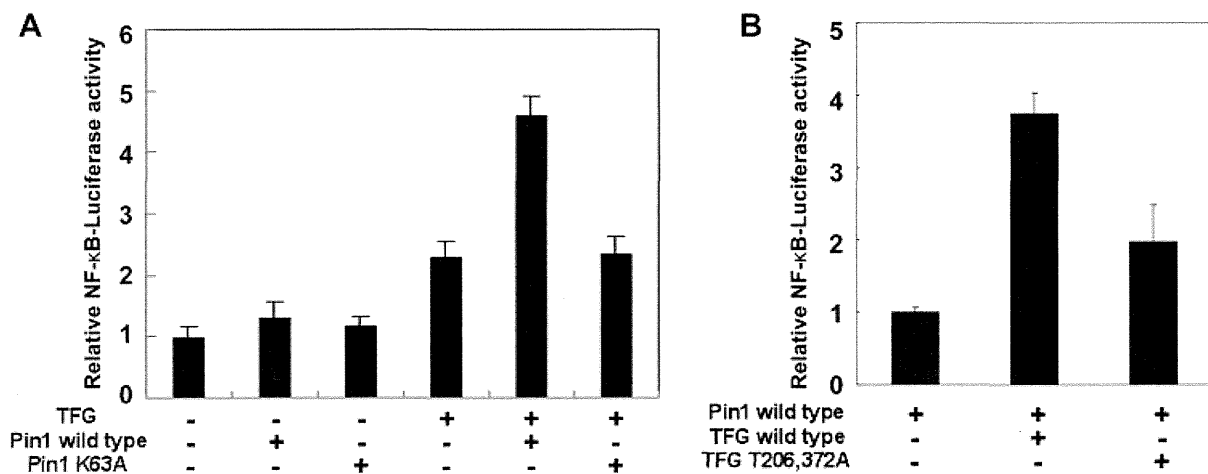


**Fig. 4.** Pin1 enhances TFG-mediated NF- $\kappa$ B activation. **A, B:** LNCaP cells were transiently transfected with the indicated plasmid vectors and co-transfected with an NF- $\kappa$ B reporter gene and pRL-TK. At 24 hr post-transfection, the cells were collected and subjected to a gene reporter assay. Immunoblots for TFG-FLAG and HA-Pin1 are shown in the upper left box. Pin1 K63A is a Pin1 mutant lacking its catalytic activity.

an AR ligand dihydrotestosterone (DHT) (Fig. 5A). Immunoprecipitation analysis revealed that TFG can specifically bind to AR (Fig. 5B). Immunofluorescent analysis further revealed that the subcellular localization of AR shifts from being cytoplasmic only to a nuclear and cytoplasmic pattern when TFG is overexpressed (Fig. 5C). These results together indicate that TFG associates with AR and thereby enhances the transcriptional activity of AR.

#### The Suppression of TFG Affects Cell Growth and Morphology

The above results indicated that TFG is a putative Pin1 substrate and plays an important role in oncogenicity in prostate cancer. We next addressed whether the specific depletion of TFG in prostate cancer cells has any effect on cell proliferation and tumorigenicity. For this purpose, we constructed two different siRNAs that target TFG and used the prostate cancer cell lines PC3, DU145, and LNCaP in which TFG has been shown to be highly overexpressed (Fig. 2A and B). As shown in Figure 6A, TFG protein levels were significantly reduced in cells treated with TFG-siRNAs when compared with control siRNA treated cells.

We next evaluated the effects of TFG depletion on *in vitro* cell growth and morphology. The suppression of TFG resulted in a substantially decreased cell growth (Fig. 6B). Morphological analysis also revealed that cells expressing TFG-siRNAs were relatively larger and contained vacuolated nuclei and a granular cytoplasm, thus showing specific features of senescent cells. Senescence-associated beta galactosidase

staining (SABG) of these cells further revealed significant increases in the number of SABG-positive cells in the TFG-siRNA population, but not in the control siRNA cells (Fig. 6C and D). These results indicate that the loss of TFG expression affects both cell proliferation and morphology by partly inducing cellular senescence in prostate cancer cells.

#### The Association Between TFG Expression and Prostate Cancer Recurrence

We next investigated the relationship between TFG expression levels and cancer recurrence. The Kaplan-Meier Method and log rank test were used to compare the significance of the recurrence free curves between two groups among 29 prostate cancer samples taken from patients after a radical prostatectomy. The results indicated a strong association between TFG expression and tumor recurrence (Fig. 7A). However, there were no such association between cancer recurrence and age, pre-operative PSA, Gleason score, or UICC stage (Fig. 7B-E). These relationships were also confirmed using the multi-variate analysis between the TFG expression levels and recurrence-free survival times (Table II).

We also investigated the relationship between TFG expression level and Age, Pre-operative PSA, Gleason score, or UICC stage among 29 prostate cancer samples taken from patients after prostatectomy (Fig. 8). There was no significant relevance between TFG expression levels and these parameters. These results demonstrate that TFG expression in prostate cancer tissues may predict a high risk of recurrence after a prostatectomy.

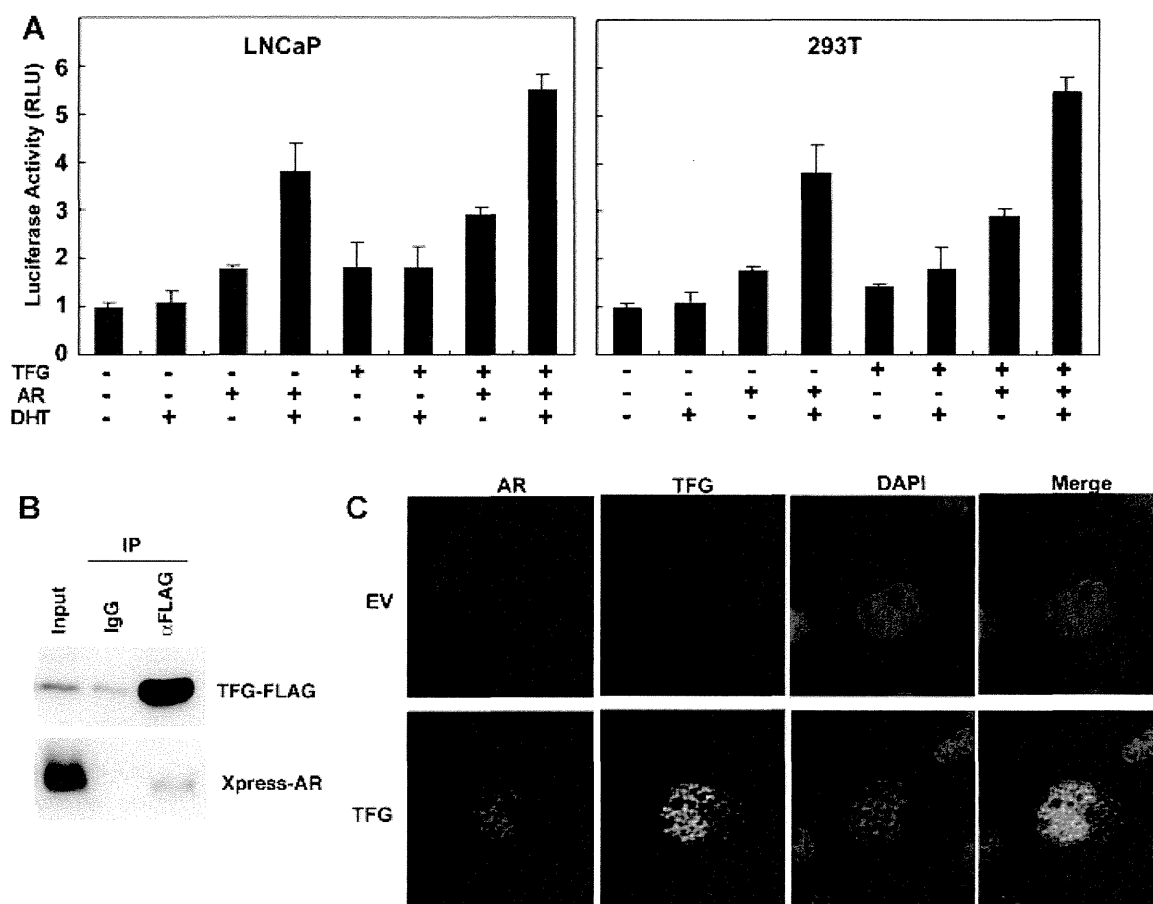


**Fig. 5.** Effects of TFG on prostate specific antigen (PSA) promoter activity. **A:** A luciferase reporter assay using a PSA promoter containing androgen responsive elements (AREs) was performed in LNCaP and 293T cells co-transfected with AR or TFG. Total DNA content was kept constant in all wells. Cells were treated or untreated with 10 nM dihydro-testosterone (DHT). **B:** 293T cells were co-transfected with TFG-FLAG and Xpress-AR. After 24 hr, cells were lysed and subjected to immunoprecipitation analysis with either rabbit anti-FLAG polyclonal antibody or non-immunized rabbit IgG (IgG). Immunoprecipitates were then processed for immunoblotting analysis with either anti-FLAG or anti-Xpress monoclonal antibodies. **C:** COS7 cells were transfected with Xpress-tagged AR and co-transfected with either TFG-FLAG or empty vector (EV). After 24 hr, cells were fixed and immunostained with anti-Xpress (Red) and anti-FLAG antibodies (Green) followed by confocal microscopy. Cell nuclei were counterstained with DAPI (blue).

## DISCUSSION

In our present study, we demonstrate that TFG is a novel Pin1-binding phosphorylated protein in prostate cancer. TFG was found to be highly expressed in prostate cancers and its expression level was closely associated with a high tumor recurrence. Furthermore, TFG activates NF-kappaB and AR signaling and a targeted TFG depletion by specific siRNA prevents cell proliferation and induces cellular senescence in prostate cancer cells. Our current Pin1-based proteomics analysis has thus revealed that TFG could be a new potential diagnostic/prognostic marker and anti-cancer target.

Ayala et al. [22] have reported that Pin1 expression is highly correlated with a higher probability of recurrence in prostate cancer after a prostatectomy.

Another report has shown that a Pin1 scoring system which sums both the nuclear and cytoplasmic grade can predict the prognosis of prostate cancer patients after a prostatectomy [23]. We have previously shown in our laboratory that Pin1 plays an important role not only in tumorigenesis but also in the maintenance of the transformed phenotype in prostate cancer cells [20]. However, Pin1 target proteins in prostate cancer have not been reported till date, and the underlying molecular mechanism has remained elusive. To address these questions, we performed Pin1-mediated proteome analyses and identified TFG as a novel Pin1 binding protein in prostate cancer cells. TFG binds Pin1 specifically in prostate cancer cells, and this interaction increases according to the degree of malignancy in Dunning rat sublines. We further found that TFG is overexpressed in prostate cancer cells or

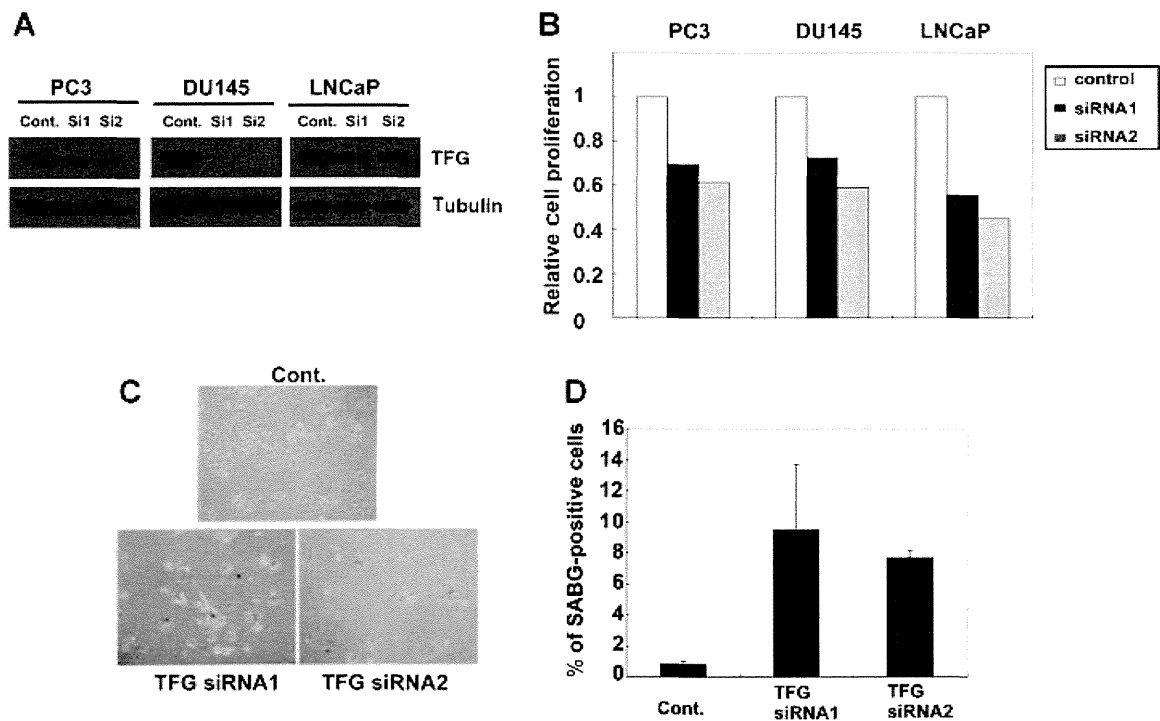


**Fig. 6.** TFG depletion inhibits cell growth in prostate cancer cells and induces cellular senescence. **A, B:** PC3, DU145, and LNCaP cells were transduced with control-siRNA (Cont) or two different TFG siRNAs (siRNA1, siRNA2) for 96 hr. Cell lysates were extracted and then subjected to immunoblot analysis with indicated antibodies (A). Cell proliferation was assessed by the MTT assay 96 hr after siRNA transfection and the figure represents the mean of three independent experiments (B). **C:** PC3 cells transduced with the indicated siRNA were subjected to senescence-associated  $\beta$ -galactosidase (SABG) staining (blue). The average number of SABG-positive cells is depicted in (D).

tissues and that its inhibition results in the suppression of cell proliferation and the induction of premature senescence in these cells. In addition, Pin1 promotes TFG-mediated NF-kappaB activation by interacting with TFG on Thr206-Pro and Thr372-Pro motifs. These results indicate that Pin1 is a positive regulator of prostate cancer malignancy through TFG-mediated NF-kappaB activation.

A previous report indicates that TFG is an uncharacterized protein that associates with NEMO and TANK to enhance NF-kappaB activity [21]. TFG was shown also here to activate AR transcriptional activity suggesting that it may engage in the hormone dependency of recurrent prostate cancer. Consistent with this hypothesis, we found in our current experiments that TFG expression positively correlates with a higher rate of tumor recurrence after radical prostatectomy. These data suggest that TFG plays an important role in prostate cancer tumorigenesis by facilitating the intracellular signaling mediated by NF-kappaB and AR. Further analysis will be required to more fully characterize the collaborative actions of Pin1 and TFG during oncogenesis. Cell growth is reduced by extracellular signals including cytokines, apoptosis induction caused by DNA damage, and cell cycle arrest via cellular senescence [24,25]. We have

reported previously that the suppression of Pin1 results in a substantial decrease of cell growth and the onset of specific features of senescence in prostate cancer cells [20]. In our present study, we demonstrate that the suppression of TFG results in a phenotype that is similar to when Pin1 is suppressed in prostate cancer cells.

To predict clinical outcomes in prostate cancer patients, the Gleason grade and/or PSA test are commonly used. These are standard clinicopathological parameters that can be useful in defining the clinical stage of prostate cancer. However, these parameters cannot predict the clinical outcome of prostate cancer patients with a moderate Gleason score (GS6 or GS7) [5] and a more precise predictive marker is thus desirable. Our current data suggest that TFG could be a potent and independent biomarker for recurrent prostate cancers and might therefore be a potential future therapeutic target.

## CONCLUSIONS

This study reveals the potential utility of Pin1 as a molecular probe that can be used to screen prostate cancer specific phosphorylated proteins. This approach has identified TFG as a new Pin1 binding

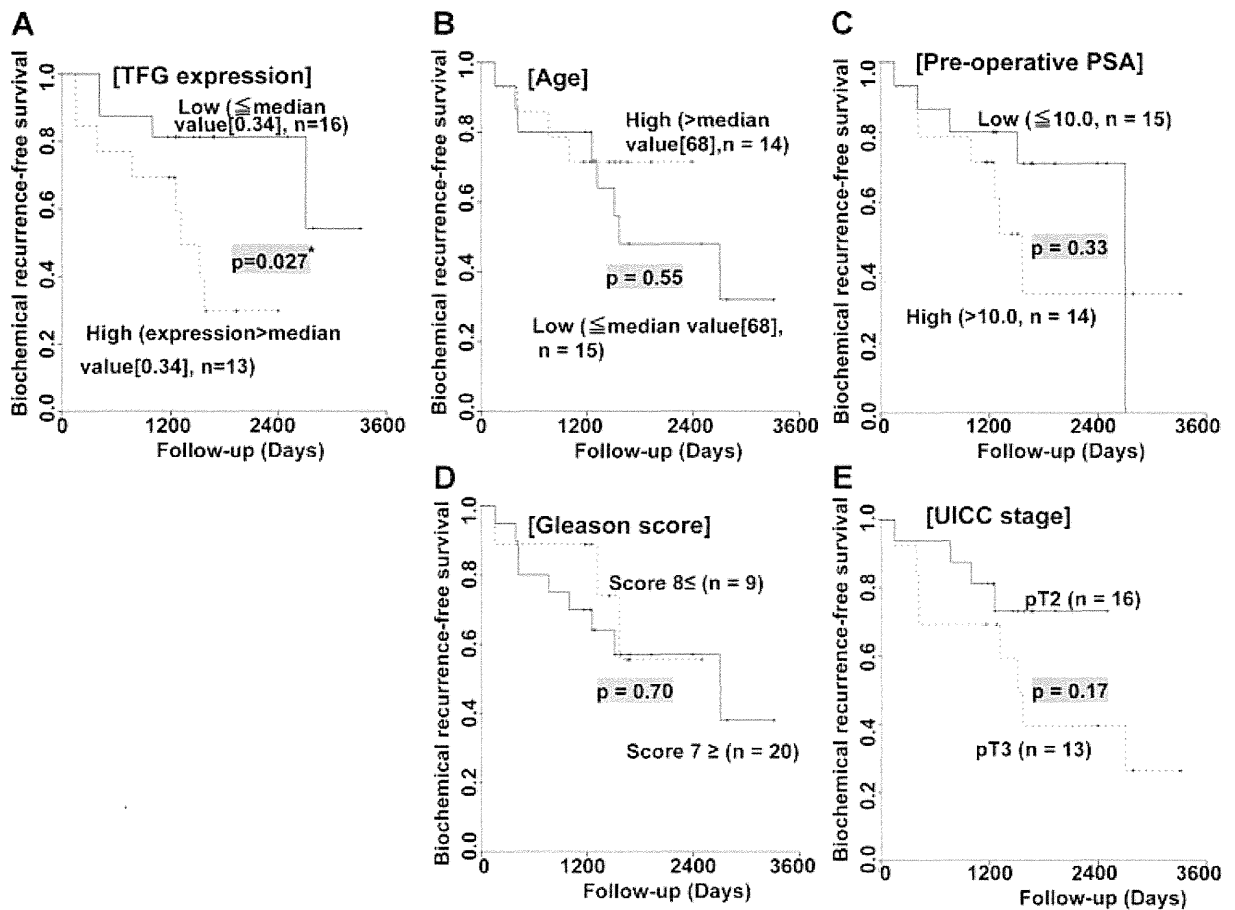


**Fig. 7.** Association between TFG expression and prostate cancer recurrence. **A–E:** Association of TFG expression levels (A), Age (B), Pre-operative PSA (C), Gleason score (D), or UICC stage (E) with recurrence-free survival. The Kaplan–Meier method and Log rank test were performed in prostate cancers (n = 29) with each parameter.  $P \leq 0.05$  indicates statistical significance. (\*:  $P < 0.05$ ).

**TABLE II. Relative Hazard of Recurrence Free Survival in Multivariate Analysis**

		HR	95% CI	P
TFG expression				
Low expression ( $\leq 0.34$ )	(n = 16)			
High expression ( $0.34 <$ )	(n = 13)	4.35	1.08–17.58	0.04*
Pre-operative PSA (ng/ml)				
$\leq 10.0$	(n = 15)			
$10.0 <$	(n = 14)	1.8	0.45–7.12	0.41
Gleason score				
$\leq 7$	(n = 20)			
$8 \leq$	(n = 9)	0.53	0.11–2.56	0.43
UICC stage				
pT2	(n = 16)			
pT3	(n = 13)	1.86	0.48–7.20	0.37
Age (years)				
$\leq 68$	(n = 15)			
$68 <$	(n = 14)	0.79	0.18–3.52	0.75

HR, hazard ratio; 95% CI, 95% confidence interval.

\*:  $P < 0.05$ .

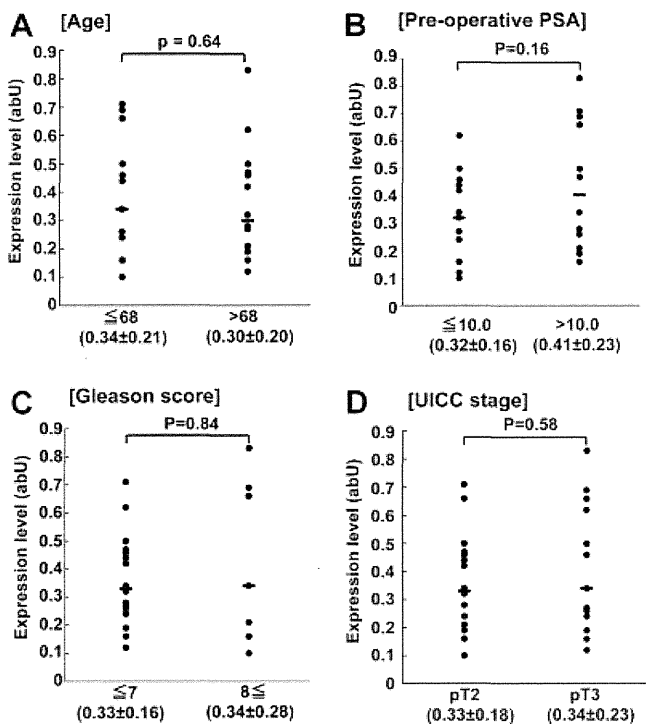


**Fig. 8.** Association between TFG expression and clinical parameters. **A–D:** Association of the TFG expression levels with Age (A), Pre-operative PSA (B), Gleason score (C), or UICC stage (D). Real-time quantitative PCR was carried out as described in Material and Methods section. Numerical values below columns indicate mean  $\pm$  standard deviation. *P*-values were calculated by Mann–Whitney *U*-test.  $P \leq 0.05$  indicates statistical significance.

protein in prostate cancer cell lines. TFG was shown to enhance the activity of both NF- $\kappa$ B and AR, presumably thereby contributing to prostatic oncogenesis. TFG expression shows a strong association with prostate cancer recurrence after prostatectomy. Our current data therefore indicate that TFG is a potential therapeutic target for prostate cancer and a biomarker for tumor recurrence.

#### ACKNOWLEDGMENTS

The authors thank T. Terada, T. Satoh (Sugiura), K. Miyoshi, and A. Kuwano for constructive advice and assistance.

#### REFERENCES

- Jemal A, Siegel R, Xu J, Ward E. Cancer statistics. *CA Cancer J Clin* 2010;60(5):277–300.
- Schroder FH, van der Crujisen-Koeter I, de Koning HJ, Vis AN, Hoedemaeker RF, Kranse R. Prostate cancer detection at low prostate specific antigen. *J Urol* 2000;163(3):806–812.
- Abate-Shen C, Shen MM. Molecular genetics of prostate cancer. *Genes Dev* 2000;14(19):2410–2434.
- De Marzo AM, DeWeese TL, Platz EA, Meeker AK, Nakayama M, Epstein JI, Isaacs WB, Nelson WG. Pathological and molecular mechanisms of prostate carcinogenesis: Implications for diagnosis, detection, prevention, and treatment. *J Cell Biochem* 2004;91(3):459–477.
- Roberts WW, Bergstralh EJ, Blute ML, Slezak JM, Carducci M, Han M, Epstein JI, Eisenberger MA, Walsh PC, Partin AW. Contemporary identification of patients at high risk of early prostate cancer recurrence after radical retropubic prostatectomy. *Urology* 2001;57(6):1033–1037.
- Upreti M, Galitovskaya EN, Chu R, Tackett AJ, Terrano DT, Granell S, Chambers TC. Identification of the major phosphorylation site in Bcl-xL induced by microtubule inhibitors and analysis of its functional significance. *J Biol Chem* 2008;283(51):35517–35525.
- Kirkland PA, Humbard MA, Daniels CJ, Maupin-Furlow JA. Shotgun proteomics of the haloarchaeon *Haloferax volcanii*. *J Proteome Res* 2008;7(11):5033–5039.
- Smal C, Vertommen D, Bertrand L, Ntamashimikiro S, Rider MH, Van Den Neste E, Bontemps F. Identification of in vivo phosphorylation sites on human deoxycytidine kinase. Role of Ser-74 in the control of enzyme activity. *J Biol Chem* 2006;281(8):4887–4893.
- Fang B, Haura EB, Smalley KS, Eschrich SA, Koomen JM. Methods for investigation of targeted kinase inhibitor therapy using chemical proteomics and phosphorylation profiling. *Biochem Pharmacol* 2010;80(5):739–747.
- Kuramitsu Y, Taba K, Ryozaawa S, Yoshida K, Zhang X, Tanaka T, Maehara S, Maehara Y, Sakaida I, Nakamura K. Identification of up- and down-regulated proteins in gemcitabine-resistant pancreatic cancer cells using two-dimensional gel electrophoresis and mass spectrometry. *Anticancer Res* 2010;30(9):3367–3372.
- Schutkowski M, Bernhardt A, Zhou XZ, Shen M, Reimer U, Rahfeld JU, Lu KP, Fischer G. Role of phosphorylation in determining the backbone dynamics of the serine/threonine-proline motif and Pin1 substrate recognition. *Biochemistry* 1998;37(16):5566–5575.
- Ryo A, Suizu F, Yoshida Y, Perrem K, Liou YC, Wulf G, Rottapel R, Yamaoka S, Lu KP. Regulation of NF- $\kappa$ B signaling by Pin1-dependent prolyl isomerization and ubiquitin-mediated proteolysis of p65/RelA. *Mol Cell* 2003;12(6):1413–1426.
- Lam PB, Burga LN, Wu BP, Hofstatter EW, Lu KP, Wulf GM. Prolyl isomerase Pin1 is highly expressed in Her2-positive breast cancer and regulates erbB2 protein stability. *Mol Cancer* 2008;7:91.
- Ryo A, Liou YC, Lu KP, Wulf G. Prolyl isomerase Pin1: A catalyst for oncogenesis and a potential therapeutic target in cancer. *J Cell Sci* 2003;116(Pt 5):773–783.
- Matsuura I, Chiang KN, Lai CY, He D, Wang G, Ramkumar R, Uchida T, Ryo A, Lu K, Liu F. Pin1 promotes transforming growth factor- $\beta$ -induced migration and invasion. *J Biol Chem* 2005;280(3):1754–1764.
- Cooke DB, Quarby VE, Petrusz P, Mickey DD, Der CJ, Isaacs JT, French FS. Expression of ras proto-oncogenes in the Dunning R3327 rat prostatic adenocarcinoma system. *Prostate* 1988;13(4):273–287.
- Miyakawa K, Ryo A, Murakami T, Ohba K, Yamaoka S, Fukuda M, Guatelli J, Yamamoto N. BCA2/Rabring7 promotes tetherin-dependent HIV-1 restriction. *PLoS Pathog* 2009;5(12):e1000700.

18. Cookson MS, Aus G, Burnett AL, Canby-Hagino ED, D'Amico AV, Dmochowski RR, Eton DT, Forman JD, Goldenberg SL, Hernandez J, Higano CS, Kraus SR, Moul JW, Tangen C, Thrasher JB, Thompson I. Variation in the definition of biochemical recurrence in patients treated for localized prostate cancer: The American Urological Association Prostate Guidelines for Localized Prostate Cancer Update Panel report and recommendations for a standard in the reporting of surgical outcomes. *J Urol* 2007;177(2):540–545.
19. Greene FL, Sobin LH. A worldwide approach to the TNM staging system: Collaborative efforts of the AJCC and UICC. *J Surg Oncol* 2009;99(5):269–272.
20. Ryo A, Uemura H, Ishiguro H, Saitoh T, Yamaguchi A, Perrem K, Kubota Y, Lu KP, Aoki I. Stable suppression of tumorigenicity by Pin1-targeted RNA interference in prostate cancer. *Clin Cancer Res* 2005;11(20):7523–7531.
21. Miranda C, Roccato E, Raho G, Pagliardini S, Pierotti MA, Greco A. The TFG protein, involved in oncogenic rearrangements, interacts with TANK and NEMO, two proteins involved in the NF-kappaB pathway. *J Cell Physiol* 2006;208(1):154–160.
22. Ayala G, Wang D, Wulf G, Frolov A, Li R, Sowadski J, Wheeler TM, Lu KP, Bao L. The prolyl isomerase Pin1 is a novel prognostic marker in human prostate cancer. *Cancer Res* 2003;63(19):6244–6251.
23. Sasaki T, Ryo A, Uemura H, Ishiguro H, Inayama Y, Yamanaka S, Kubota Y, Nagashima Y, Harada M, Aoki I. An immunohistochemical scoring system of prolyl isomerase Pin1 for predicting relapse of prostate carcinoma after radical prostatectomy. *Pathol Res Pract* 2006;202(5):357–364.
24. Frater-Schroder M, Risau W, Hallmann R, Gautschi P, Bohlen P. Tumor necrosis factor type alpha, a potent inhibitor of endothelial cell growth in vitro, is angiogenic in vivo. *Proc Natl Acad Sci USA* 1987;84(15):5277–5281.
25. Xu X, Fu XY, Plate J, Chong AS. IFN-gamma induces cell growth inhibition by Fas-mediated apoptosis: requirement of STAT1 protein for up-regulation of Fas and FasL expression. *Cancer Res* 1998;58(13):2832–2837.

# Heat shock protein 90 regulates phosphatidylinositol 3-kinase-related protein kinase family proteins together with the RUVBL1/2 and Tel2-containing co-factor complex

Natsuko Izumi,<sup>1,7</sup> Akio Yamashita,<sup>1,2,3,4,6</sup> Hisashi Hirano<sup>3,5</sup> and Shigeo Ohno<sup>1,3,6</sup>

<sup>1</sup>Departments of Molecular Biology, <sup>2</sup>Microbiology and Molecular Biodefense Research, School of Medicine, <sup>3</sup>Advanced Medical Research Center, Yokohama City University, Yokohama; <sup>4</sup>Precursory Research for Embryonic Science and Technology, Japan Science and Technology Agency, Kawaguchi; <sup>5</sup>International Graduate School of Arts and Sciences, Yokohama City University, Yokohama, Japan

(Received August 15, 2011/Revised September 7, 2011/Accepted September 19, 2011/Accepted manuscript online September 23, 2011/Article first published online October 24, 2011)

Heat shock protein 90 (Hsp90), a conserved molecular chaperone for a specific set of proteins critical for signal transduction including several oncogenic proteins, has been recognized as a promising target for anticancer therapy. Hsp90 inhibition also sensitizes cancer cells to DNA damage. However, the underlying mechanisms are not fully understood. Here, we provide evidence that Hsp90 is a general regulator of phosphatidylinositol 3-kinase-related protein kinase (PIKK) family proteins, central regulators of stress responses including DNA damage. Inhibition of Hsp90 causes a reduction of all PIKK and suppresses PIKK-mediated signaling. In addition, Hsp90 forms complexes with RUVBL1/2 complex and Tel2 complex, both of which have been shown to interact with all PIKK and control their abundance and functions. These results suggest that Hsp90 can form multiple complexes with the RUVBL1/2 complex and Tel2 complex and function in the regulation of PIKK, providing additional rationale for the effectiveness of Hsp90 inhibition for anticancer therapy, including sensitization to DNA damage. (*Cancer Sci* 2012; 103: 50–57)

Heat shock protein 90 (Hsp90) is an evolutionarily conserved molecular chaperone that plays a critical role in cellular homeostasis through stabilization and activation of several “client proteins” involved in a variety of cellular processes, including signal transduction, transcriptional regulation and cellular stress responses.<sup>(1,2)</sup> Hsp90 works cooperatively with the Hsp40-Hsp70 chaperone system in an ordered pathway, where Hsp90 binds to a client protein at the late stage of protein folding and facilitates its stability, structural maturation and assembly of a complex.<sup>(3)</sup> Hsp90 is an ATPase, and ATP binding/hydrolysis-driven conformational changes of Hsp90 are required for its chaperone activity.<sup>(4–6)</sup> In this Hsp90 chaperone cycle, Hsp90 forms dynamic complexes with co-chaperones/factors that regulate the Hsp90 ATPase cycle and the client interactions with Hsp90.<sup>(2,7)</sup> The dynamic and transient nature of the Hsp90 chaperone complexes and the unstable character of Hsp90 clients have hindered the establishment of a comprehensive picture of the Hsp90 chaperone system.

Geldanamycin and its derivatives, such as 17-allylamino-17-desmethoxygeldanamycin (17-AAG), compete with ATP binding and inhibit Hsp90 chaperone activity, leading to degradation of client proteins.<sup>(8,9)</sup> Importantly, these Hsp90 inhibitors selectively kill cancer cells compared to normal cells. This selectivity means that Hsp90 is a crucial facilitator of oncogene addiction and cancer cell survival and a molecular target for cancer therapy.<sup>(10)</sup> The mechanisms of the cancer selectivity of Hsp90 inhibitor are not fully understood but are partly explained by the observation that the bulk of Hsp90 exists in active Hsp90

complexes in cancer cells, whereas most Hsp90 in normal cells exists in a latent, uncomplexed state.<sup>(11)</sup> Therefore, analyses of the biochemical nature of the specific Hsp90-client complexes in cancer cells are critical for understanding of the cancer specificity of Hsp90 inhibitors.

In addition to the selective killing of cancer cells, Hsp90 inhibitors sensitize cancer cells to radiation and DNA damaging agents. Hence, the combination of the Hsp90 inhibition and radiation/DNA damaging therapeutic drugs is a promising strategy for anticancer therapy.<sup>(12,13)</sup> Although multiple mechanisms participate in the radio-sensitization caused by Hsp90 inhibition, impaired DNA repair pathways seem to be responsible for at least part of that. For example, an Hsp90 inhibitor 17-AAG blocks homologous recombination repair induced by DNA double-strand breaks (DSB) in prostate or lung cancer cells but not normal fibroblasts.<sup>(14)</sup> 17-AAG also impairs the Fanconi anemia (FA) DNA repair pathway, whose activation requires ataxia telangiectasia mutated (ATM)- and Rad3-related (ATR)-mediated phosphorylation of FANCA, one of the FA proteins.<sup>(15,16)</sup> Another Hsp90 inhibitor, 17-N-dimethylaminoethylamino-17-demethoxygeldanamycin (17DMAG), compromises the DSB repair through an impairment of ionizing radiation (IR)-responsive activation of DNA-dependent protein kinase catalytic subunit (DNA-PKcs) and ATM.<sup>(17)</sup>

The phosphatidylinositol 3-kinase-related protein kinase (PIKK) family includes ATM, DNA-PKcs and ATR, as well as suppressor with morphological effect on genitalia 1 (SMG-1), mammalian target of rapamycin (mTOR) and transformation/transcription domain-associated protein (TRRAP) in mammals. SMG-1 is an essential factor of nonsense-mediated mRNA decay (NMD), one of the mRNA quality control systems,<sup>(18,19)</sup> and TRRAP regulates transcription as a shared component of histone acetyl transferase complexes.<sup>(20)</sup> SMG-1 and TRRAP are also involved in DNA damage signaling and repair.<sup>(21–23)</sup> mTOR senses nutrient status and coordinates cellular translational activity and cell growth/proliferation.<sup>(24)</sup>

Recent studies have revealed the existence of common regulators of all PIKK members, RuvB-like 1 (RUVBL1), RUVBL2 and telomere maintenance 2 (Tel2). RUVBL1 and RUVBL2 are conserved ATPases belonging to the ATPases with associated diverse cellular activities (AAA+) family.<sup>(25)</sup> They form a complex (RUVBL1/2) and participate in diverse cellular processes, including transcription, RNA modification, telomere maintenance and DNA repair.<sup>(26)</sup> RUVBL1/2 interacts with all PIKK

<sup>6</sup>To whom correspondence should be addressed.

E-mails: ohnos@med.yokohama-cu.ac.jp; yamasita@yokohama-cu.ac.jp

<sup>7</sup>Present address: Institute of Molecular and Cellular Biosciences, University of Tokyo, Tokyo, Japan.

members and controls the PIKK abundance at least at the mRNA level.<sup>(27)</sup> RUVBL1/2 also regulates functional complex formation of SMG-1 during NMD.<sup>(27)</sup> Tel2 interacts with all PIKK and regulates the stability of PIKK proteins.<sup>(28)</sup> Tel2 also functions in the recruitment of Tel1 (ATM ortholog in *S. cerevisiae*) to DNA damage sites and the Rad3/ATR-mediated DNA damage response.<sup>(29-31)</sup> We recently found that Hsp90 inhibition causes the downregulation of PIKK members,<sup>(27)</sup> as observed for knockdown/knockout of either RUVBL1/2 or Tel2. This raises an intriguing possibility that at least a part of the Hsp90-induced sensitization to DNA damage can be attributed to the reduction and/or inactivation of these PIKK. However, it has been reported, controversially, that Hsp90 inhibition does not affect the abundance of PIKK.<sup>(17,32)</sup>

In this study, we first evaluated the effect of the Hsp90 inhibition on PIKK abundance and PIKK-mediated signaling. We confirm that Hsp90 inhibition decreases the abundance of all PIKK proteins (ATM, ATR, DNA-PKcs, mTOR, SMG-1 and TRRAP). Importantly, Hsp90 inhibition severely compromises PIKK-mediated signaling pathways. In addition, Hsp90 physically interacted with RUVBL1/2, Tel2, and their associating proteins. Both RUVBL1/2 and Tel2 interacted with two evolutionarily conserved Hsp90 co-factors, NOP17 and RPAP3. These results strongly support the notion that Hsp90 can form diverse protein complexes with RUVBL1/2 and/or Tel2, and that it acts as a general PIKK regulator.

## Materials and Methods

**Plasmids, antibodies, siRNA and inhibitor.** pcDNA5/FRT/TO/NTAP-GST and pcDNA5/FRT/TO/NTAP-SMG-10 have been described previously.<sup>(27)</sup> pcDNA5/FRT/TO/NTAP-NOP17 and pcDNA5/FRT/TO/NTAP-RPAP3 were constructed by the cloning of each cDNA fragment to the pcDNA5/FRT/TO/NTAP vector using standard methods.

Anti-Tel2 and anti-Tti2 antisera were generated against recombinant human Tel2 (aa 624–691) or human Tti2 (aa 8–

108) fused to glutathione S-transferase (GST). The anti-SMG-1, Upf1, SMG-10 and Phosho-Upf1 (clone 3B8 or 8E6) antibodies have been described previously.<sup>(19,33-35)</sup> Antibodies to Hsp90 $\alpha/\beta$  (#4874; Cell Signaling Technology, Beverly, MA, USA), RUVBL1 (#BMR00431; Biomatrix, Chiba, Japan and #sc-15259; Santa Cruz Biotechnology, Santa Cruz, CA, USA), RUVBL2 (#612482; BD Transduction Laboratories, Franklin Lakes, NJ, USA), RNA polymerase II subunit 5 (RPB5) (#S3157\_EP; Euromedex, Souffelweyersheim, France), DNA-PKcs (#A300-519A; Bethyl Laboratories, Montgomery, TX, USA), ATM (#2873; Cell Signaling Technology), ATR (#ab1; Calbiochem, Darmstadt, Germany), mTOR (#2972; Cell Signaling Technology), TRRAP (#A301-132A; Bethyl), Akt (#9272; Cell Signaling Technology), Chk1 (#sc-8408; Santa Cruz), P-Chk1 (Ser345) (#2348; Cell Signaling Technology), Chk2 (#2662; Cell Signaling Technology), P-Chk2 (Thr68) (#2661; Cell Signaling Technology), p70 S6K (#sc-230; Santa Cruz), P-p70 S6K (Thr389) (#9205; Cell Signaling Technology), P-S/TQ ATM/ATR substrate (#2851; Cell Signaling Technology), JNK (#15701A; BD Pharmingen, San Diego, CA, USA), unconventional prefoldin RPB5 interactor (URI) (#A301-164-1; Bethyl), nucleolar protein 17 (NOP17) (#H00055011-M05; Abnova, Taipei, Taiwan), RNA polymerase II associated protein 3 (RPAP3) (#H00079657-B01P; Abnova), Hsp70 (#SPA-810; Stressgen, Victoria, BC, Canada), Myosin IIa (#M8064; Sigma, St. Louis, MO, USA), GAPDH (#ab8245; Abcam, Cambridge, MA, USA), nuclear cap binding protein subunit 1, 80kDa (CBP-80) (#10349-1-AP; Protein Tech Group, Chicago, IL, USA),  $\beta$ -actin (#A1978; Sigma) and  $\alpha$ -tubulin (#T6199; Sigma) were obtained commercially.

The following siRNA target sequences were used: RUVBL1, siGENOME duplex D-008977-02 (Dharmacon, Lafayette, CO, USA); RUVBL2, siGENOME duplex D-012299-03 (Dharmacon); SMG-10, siGENOME duplex J-014188-05 (Dharmacon); Tti2, Hs\_Tti2\_2 HP Validated siRNA SI00401660 (Qiagen, Valencia, CA, USA); Tel2, Hs\_KIAA0683\_4 HP Validated siRNA SI00454909 (Qiagen); URI, Hs\_C19orf2\_4 HP

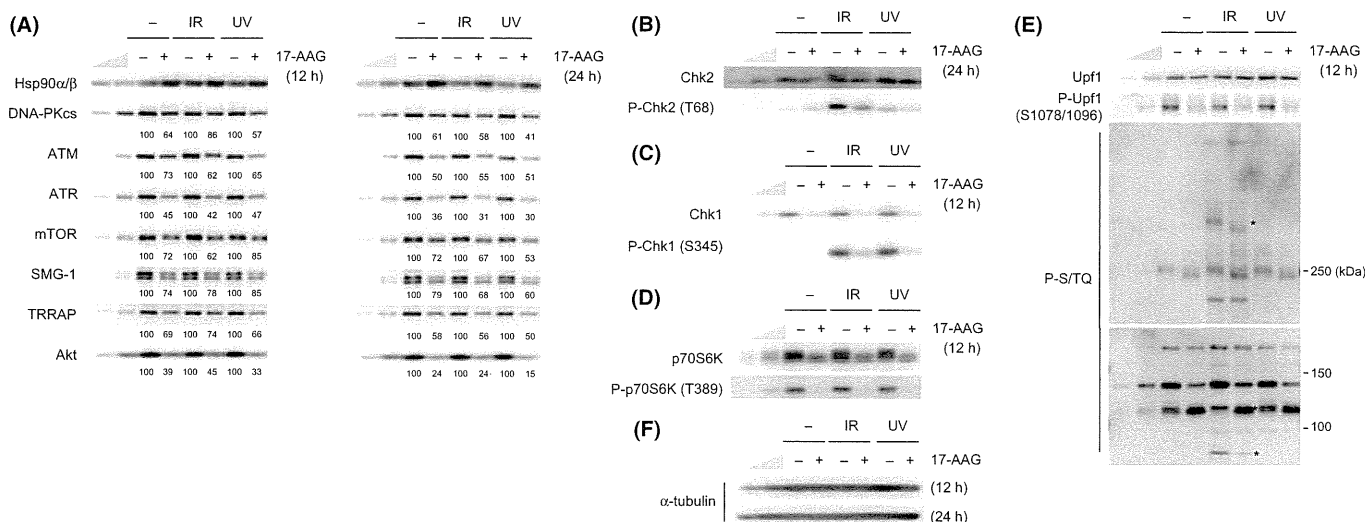


**Fig. 1.** Inhibition of heat shock protein 90 (Hsp90) activity decreases the abundance of all phosphatidylinositol 3-kinase-related protein kinase (PIKK) proteins and the downstream signaling. (A–F) HeLa TetOff cells were treated with vehicle or 2  $\mu$ M 17-allylamino-17-desmethoxygeldanamycin (17-AAG) for 12 or 24 h, then the cells were untreated, treated with 10 Gy IR, or 100 J/m<sup>2</sup> of UV, and incubated for 1 h. Total cell lysates were analyzed by western blotting with the indicated antibodies. To estimate the protein abundance, 33 and 11% of the 17-AAG, IR and UV-untreated samples were loaded. The anti-P-S/TQ antibody recognizes phosphorylated serine or threonine in the SQ motif, potential phosphorylation sites by ATM/ATR/SMG-1/DNA-PKcs (E, lower panel). Asterisks indicate some examples of phosphoproteins affected by the 17-AAG treatment (E, lower panel). ATM, ataxia telangiectasia mutated; ATR, ATM-and Rad3-related; DNA-PKcs, DNA-dependent protein kinase catalytic subunit; mTOR, mammalian target of rapamycin; SMG-1, suppressor for morphological effect on genitalia 1; TRRAP, transformation/transcription domain-associated protein.



Validated siRNA SI00322462 (Qiagen); RPB5, Hs\_POLR2E\_3 HP Validated siRNA SI00689073 (Qiagen); NOP17, Hs\_FLJ20643\_4 HP Validated siRNA SI00120148 (Qiagen); RPAP3, Hs\_FLJ21908\_3 HP Validated siRNA SI00399875 (Qiagen); DNA-PKcs, #1: Hs\_PRKDC\_8\_HP Validated siRNA SI02663633 (Qiagen), #2: Hs\_PRKDC\_2\_HP Validated siRNA SI00093079 (Qiagen); ATM, #1: Hs\_ATM\_4\_HP Validated siRNA SI00000847 (Qiagen), #2: Hs\_ATM\_14\_HP Validated siRNA SI03068506 (Qiagen); ATR, #1: Hs\_ATR\_12\_HP Validated siRNA SI02664347 (Qiagen), #2: Hs\_ATR\_2\_HP Validated siRNA SI00023107 (Qiagen); mTOR, #1: Hs\_FRAP1\_7\_HP Validated siRNA SI03023587 (Qiagen), #2: Hs\_FRAP1\_8\_HP Validated siRNA SI03064985 (Qiagen); SMG-1, #1: Mm\_2610207I05Rik\_4 HP Validated siRNA SI02765546 (Qiagen), #2: GTGTATGTGCGCCAAAGTA; TRRAP, #1: Hs\_TRRAP\_2\_HP Validated siRNA SI00052591 (Qiagen), #2: Hs\_TRRAP\_3\_HP Validated siRNA SI00052598 (Qiagen); and NS siRNA, All Star Negative Control siRNA (Qiagen).

17-allylamino-17-desmethoxygeldanamycin (17-AAG) (Sigma) was used.

**Cell culture and transfection.** HeLa TetOff cells (TaKaRa Clontech, Shiga, Japan) and Flp-In T-Rex HEK293 cells (Invitrogen, Carlsbad, CA, USA) were grown in DMEM supplemented with 10% FBS, 100 U/mL penicillin and 100 µg/mL streptomycin.

Tet-inducible SBP streptavidin binding peptide (SBP)-tagged FlpIn T-Rex HEK 293 stable cells have been described previously.<sup>(27)</sup> siRNA transfections were performed in 12-well or 6-well plates using siLentFect (BioRad, Hercules, CA, USA) according to the manufacturer's protocol, and cells were harvested 60 h later. Plasmid transfections were performed in 15-cm dishes using Lipofectamine LTX (Invitrogen), according to the manufacturer's protocol, and cells were harvested 36 h later.

**Affinity purification and mass spectrometry.** Affinity purification and mass spectrometry analysis were performed as described previously.<sup>(27)</sup>

**Immunoprecipitation and western blot analysis.** HeLa TetOff cells were lysed in T-buffer (20 mM Hepes-NaOH at pH 7.5, 150 mM NaCl, 0.05% Tween 20, 2.5 mM MgCl<sub>2</sub>, 0.5 mM DTT, 100 nM okadaic acid [Calbiochem], protease inhibitor cocktail [Roche Applied Science, Indianapolis, IN, USA], phosphatase inhibitor cocktail [Roche] and 100 µg/mL RNaseA [Qiagen]). The soluble fractions were incubated with antibodies for 1 h at 4°C with gentle rotation. Subsequently, the soluble fractions were incubated with Dynabeads protein G (Invitrogen) for an additional 1 h at 4°C with gentle rotation. After washing with RNase(-) lysis buffer, the immunocomplexes were boiled in SDS sample buffer, and analyzed by western blotting. All proteins in western blot experiments were detected with Lumi-

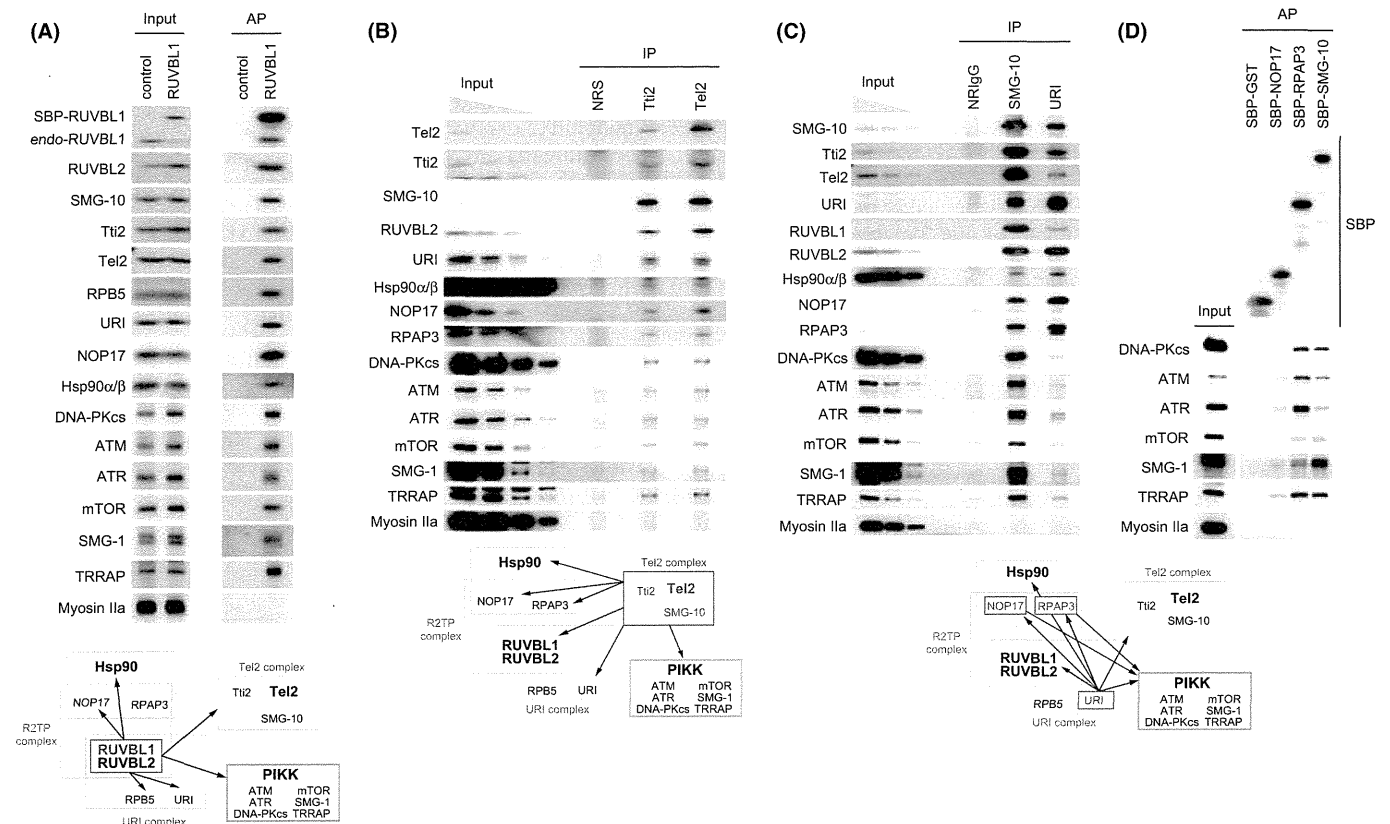


**Fig. 2.** Heat shock protein 90 (Hsp90) interacts with two other phosphatidylinositol 3-kinase-related protein kinase (PIKK) regulators, RUVBL1/2 and Tel2 and their associated proteins. (A) RUVBL1 interacted with Hsp90, a Hsp90 co-factor (NOP17), URI complex and Tel2 complex. Tet-inducible streptavidin-binding peptide (SBP)-tagged RUVBL1 stable HEK 293 cells or control cells, which express tag peptides only, were treated with 1 ng/mL doxycycline for 3 days. Cytoplasmic cell extracts were affinity purified with streptavidin sepharose, and biotin-eluted fractions were analyzed by western blotting with the indicated antibodies. (B,C) Protein interactions of Tel2, SMG-10, Tti2 and URI. HeLa TetOff cells were immunoprecipitated with anti-Tti2, anti-Tel2 antiserum or normal rabbit serum (NRS) (B), or anti-SMG-10, URI, or normal rabbit IgG (NRlgG) (C). The immunoprecipitates were analyzed by western blotting with the indicated antibodies. (D) RPAP3 interacts with all PIKK. HeLa TetOff cells were transfected with pcDNA5/FRT/TO/NTAP-GST, pcDNA5/FRT/TO/NTAP-NOP17, pcDNA5/FRT/TO/NTAP-RPAP3 or pcDNA5/FRT/TO/NTAP-SMG-10. The cell extracts were subjected to affinity purification with streptavidin sepharose 36 h later and analyzed by western blotting with indicated antibodies. ATM, ataxia telangiectasia mutated; ATR, ATM-and Rad3-related; DNA-PKcs, DNA-dependent protein kinase catalytic subunit; mTOR, mammalian target of rapamycin; NOP17, nucleolar protein 17; RPB5, RNA polymerase II subunit 5; SMG-1, suppressor with morphological effect on genitalia 1; TRRAP, transformation/transcription domain-associated protein.

Light plus western blotting substrate (Roche) or Immobilon Western (Millipore, Billerica, MA, USA) and quantified with a Lumino-Imager, LAS-3000, and Science Lab 2001 Image Gauge software (Fuji Photo Film, Tokyo, Japan).

## Results

**Heat shock protein 90 inhibition causes reduction of all phosphatidylinositol 3-kinase-related protein kinase and phosphatidylinositol 3-kinase-related protein kinase-mediated stress signaling.** To re-examine the role of Hsp90 on the abundance of PIKK proteins, we treated HeLa TetOff cells with 17-AAG, an Hsp90 inhibitor, and incubated for 12 or 24 h. We showed that Hsp90 inhibition caused apparent downregulation of ATM, ATR and DNA-PKcs (Fig. 1A). The different effect of Hsp90 inhibition on PIKK abundance from previous reports might reflect the difference in sensitivity to Hsp90 of each cell line.<sup>(17,32)</sup> Moreover, the Hsp90 inhibition attenuates IR-induced Chk2 phosphorylation at Thr68, which is mediated by ATM and induces cell cycle checkpoint to response DNA damage (Fig. 1B). In addition, IR-induced phosphorylations of putative ATM/ATR substrates were decreased under the Hsp90 inhibition (Fig. 1E, lower panel). Consistent with these results, the inhibition of Hsp90 mediates impairment of IR-induced cell cycle checkpoints and significant delay of DNA repair.<sup>(17)</sup> Furthermore, Hsp90 inhibition reduced the protein amount of other PIKK, mTOR, SMG-1 and TRRAP (Fig. 1A). In addition, suppression of ATR-mediated Chk1 phosphorylation at Ser345 accompanied by a significant reduction of Chk1 was observed, which is consistent with a previous study (Fig. 1C).<sup>(36)</sup> These results suggest that at least a part of the sensitization to DNA damage caused by Hsp90 inhibition results from the reduction of PIKK and impaired PIKK-mediated DNA damage responses. We further investigated the effects of Hsp90 inhibition on mTOR-mediated or SMG-1-mediated signaling. mTOR controls cell size/proliferation and translation activity in response to the nutrient status through the phosphorylation of p70S6 kinase.<sup>(24)</sup> The Hsp90 inhibition reduced the mTOR-mediated phosphorylation of p70S6 kinase at Thr389, with moderate reduction of p70S6 kinase (Fig. 1D). Because mTOR is activated by Akt, one of the Hsp90 clients shown in Figure 1A, we cannot exclude the possibility that the reduced phosphorylation of p70S6 kinase is a consequence of the downregulation of Akt. The SMG-1-mediated Upf1 phosphorylation at Ser1078/1096 is essential for nonsense-mediated mRNA decay, a quality control system that selectively degrades aberrant mRNA with premature termination codons.<sup>(18)</sup> The Hsp90 inhibition obviously decreased the SMG-1-mediated Upf1 phosphorylation (Fig. 1E, upper panel). No apparent reduction of  $\alpha$ -tubulin was observed with the Hsp90 inhibition (Fig. 1F). Taken together, these results indicate that Hsp90 is required for the maintenance of all PIKK proteins and PIKK signaling.

**Heat shock protein 90 physically interacts with the common regulators of phosphatidylinositol 3-kinase-related protein kinase, RUVBL1/2 and Tel2.** Previous studies have revealed that PIKK members can be regulated by common factors, the RUVBL1 and RUVBL2 complex (RUVBL1/2) and Tel2.<sup>(27,28)</sup> The physical interactions between RUVBL1 and Hsp90 and between RUVBL1 and Tel2 led us to hypothesize that Hsp90 is involved in the PIKK regulation together with RUVBL1/2 and/or Tel2.<sup>(27)</sup> To evaluate this possibility, we examined physical interactions among Hsp90, RUVBL1/2 and Tel2.

We confirmed co-purification of Hsp90 with RUVBL1 from a HEK 293-cell extract stably expressing SBP-tagged RUVBL1 (Fig. 2A).<sup>(27)</sup> In addition, endogenous Tel2 co-immunoprecipitated Hsp90 from HeLa TetOff cell extract (Fig. 2B). Tel2 form an evolutionally conserved complex with SMG-10 (also known as Tti1) and Tti2.<sup>(37-39)</sup> In our experiments, tight associations among Tel2, SMG-10 and Tti2 were also observed (Fig. 2B,C). As with Tel2, both SMG-10 and Tti2 co-immunoprecipitated RUVBL1/2 and Hsp90, indicating that the Tel2 complex associates with RUVBL1/2 and Hsp90 (Fig. 2B,C).

RUVBL1/2 has been identified in a complex named R2TP, containing Tah1 (RPAP3 in mammals) and Pih1 (NOP17 in mammals),<sup>(40)</sup> and URI-prefoldin complex together with RPB5 (see the schemes in Fig. 2).<sup>(41)</sup> Because the Tel2 complex com-

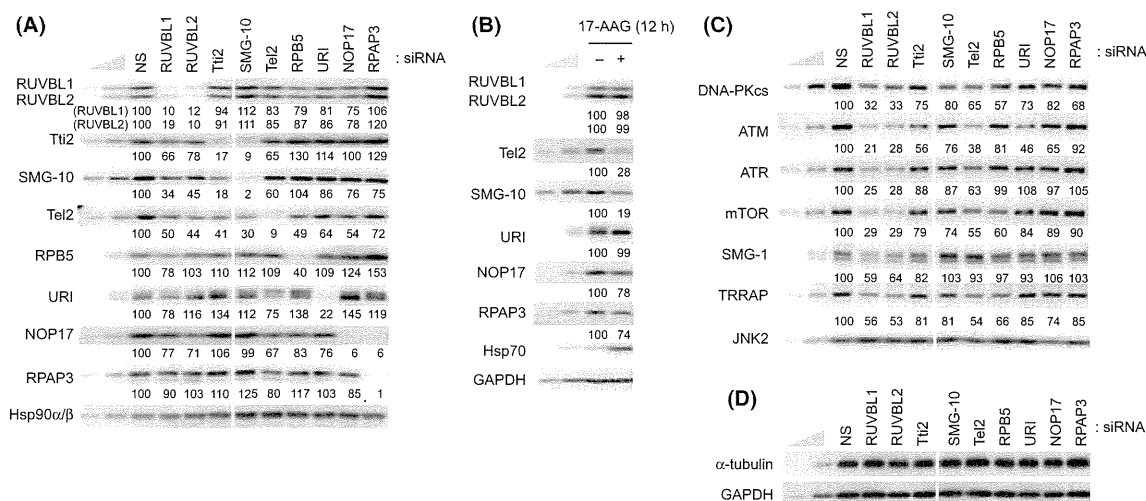


**Fig. 3.** Knockdown of RUVBL1/2 and Tel2 interacting proteins partially affects the phosphatidylinositol 3-kinase-related protein kinase (PIKK) abundance. (A,C,D) HeLa TetOff cells were transfected with the indicated siRNA. Sixty hours after transfection, total cell lysates were analyzed by western blotting with the indicated antibodies. Same knockdown samples were used in panels A, C, D in Figure 3, and panels A and B in Figure 4. Mean values of the relative protein levels compared to the nonsilencing (NS) control from two independent experiments are shown under the blots. (B) HeLa TetOff cells were treated with vehicle or 2  $\mu$ M 17-AAG for 12 h and total cell lysates were analyzed by western blotting with the indicated antibodies. To estimate the protein abundance, 33 and 11% of the NS sample (A,C,D) or untreated sample (B) were loaded. ATM, ataxia telangiectasia mutated; ATR, ATM and Rad3-related; DNA-PKcs, DNA-dependent protein kinase catalytic subunit; mTOR, mammalian target of rapamycin; SMG-1, suppressor with morphological effect on genitalia 1; TRRAP, transformation/transcription domain-associated protein.

ponents interact with RUVBL1, as confirmed in Figure 2A, we probed the antibodies against these RUVBL1 interacting proteins,<sup>(27,42)</sup> NOP17, RPAP3, RPB5 and URI, for the purified RUVBL1 complex and Tel2, SMG-10 or Tti2 immunoprecipitates. As expected, all of them co-purified and co-immunoprecipitated with SBP-RUVBL1 and endogenous Tel2, SMG-10 and Tti2, respectively (Fig. 2A–C). To confirm these protein interactions, endogenous URI immunoprecipitate from HeLa TetOff cell extract was analyzed. As shown in Figure 2C, URI co-immunoprecipitated with Hsp90, RUVBL1/2, Tel2, and their interacting proteins. These results indicate that Hsp90, RUVBL1/2, Tel2, SMG-10, Tti2, NOP17, RPAP3 and URI can physically interact and form complexes.

Because both RUVBL1/2 and Tel2 are common PIKK binding proteins, we investigated whether RUVBL1/2-interacting and Tel2-interacting proteins also associate with PIKK. We probed PIKK antibodies to purified SBP-RUVBL1 complexes (Fig. 2A), immunoprecipitates of endogenous Tel2, Tti2 (Fig. 2B), SMG-10 and URI (Fig. 2C), and purified SBP-NOP17, PARP3 and SMG-10 complexes (Fig. 2D). The results indicate that all protein tested in this study can interact with all PIKK, although the significances differ among precipitated proteins (Fig. 2). Taken together, Hsp90, RUVBL1/2, Tel2, SMG-10, Tti2, NOP17, RPAP3 and URI can physically interact with PIKK, probably as a part of complex.

**RUVBL1/2, Tel2 and their associated proteins are involved in phosphatidylinositol 3-kinase-related protein kinase signaling.** The physical association of the RUVBL1/2-associated and Tel2-associated proteins with PIKK suggests the possibility that they are involved in the regulation of PIKK abundance and/or PIKK signaling, like RUVBL1/2 and Tel2. To test this, we analyzed knockdown effects of each molecule. As shown in Figure 3A, the siRNA efficiently knocked down each molecule. We found close relationships among RUVBL1/2, Tel2 and their associated proteins (Fig. 3A). For instance, SMG-10 and Tti2 interdependently regulated the other protein abundance. NOP17 also depended on RPAP3 for its abundance. Knockdown of RUVBL1, RUVBL2 or Tel2 also decreased the abundance of SMG-10, Tti2 and NOP17. NOP17 was also reduced by the knockdown of Tel2. Tel2 was decreased by the knockdown of RUVBL1, RUVBL2, SMG-10, Tti2, RPB5 or NOP17. The abundance of RUVBL1 and RUVBL2 was decreased to <50% by the knockdown of RPB5 or NOP17. These observations indicate an interdependent relationship among RUVBL1/2, Tel2 and their associated proteins. It might reflect the change of their protein stability, based on the previous reports.<sup>(38,43)</sup>

In addition, Hsp90 inhibition clearly decreased the abundance of Tel2 and SMG-10 (Fig. 3B), suggesting a possibility that the Tel2 complex components are Hsp90 clients. Note that any knockdown of RUVBL1/2-associated and Tel2-associated proteins did not decrease the abundance of Hsp90 (Fig. 3A).

Consistent with previous reports, knockdown of RUVBL1, RUVBL2 or Tel2 decreased the abundance of PIKK (Fig. 3C).<sup>(27,28)</sup> However, a slight reduction of DNA-PKcs and ATM was observed by the knockdown of Tti2, SMG-10, URI or NOP17 in this transient knockdown experiment (Fig. 3C). Long-term knockdown of SMG-10 or Tti2 probably results in the downregulation of all PIKK, as reported in recent report.<sup>(38)</sup> RPB5 knockdown also modestly affects the abundance of DNA-PKcs, mTOR and TRRAP; however, it might influence transcription activity, given that RPB5 is an RNA polymerase subunit (Fig. 3C).<sup>(44)</sup>

In contrast, knockdown of RUVBL1/2-associated and Tel2-associated proteins partially affected PIKK signaling. For example, the relative level of the mTOR-mediated phosphorylation of p70S6 kinase at Thr389 without additional stimulation was decreased by the knockdown of URI, NOP17 or RPAP3, in addition to the knockdown of RUVBL1 or RUVBL2 (Fig. 4A).

The relative level of SMG-1-mediated Upf1 phosphorylation at Ser1078/1096 was reduced only by the RUVBL1, RUVBL2 or RPB5 knockdown but not affected by others (Fig. 4B). However, the phosphorylation of a 140-kDa protein detected by a phospho-S/TQ antibody, which recognizes phosphorylated ATM/ATR substrates, was reduced by the knockdown of Tti2 and SMG-10, in addition to the knockdown of RUVBL1, RU-

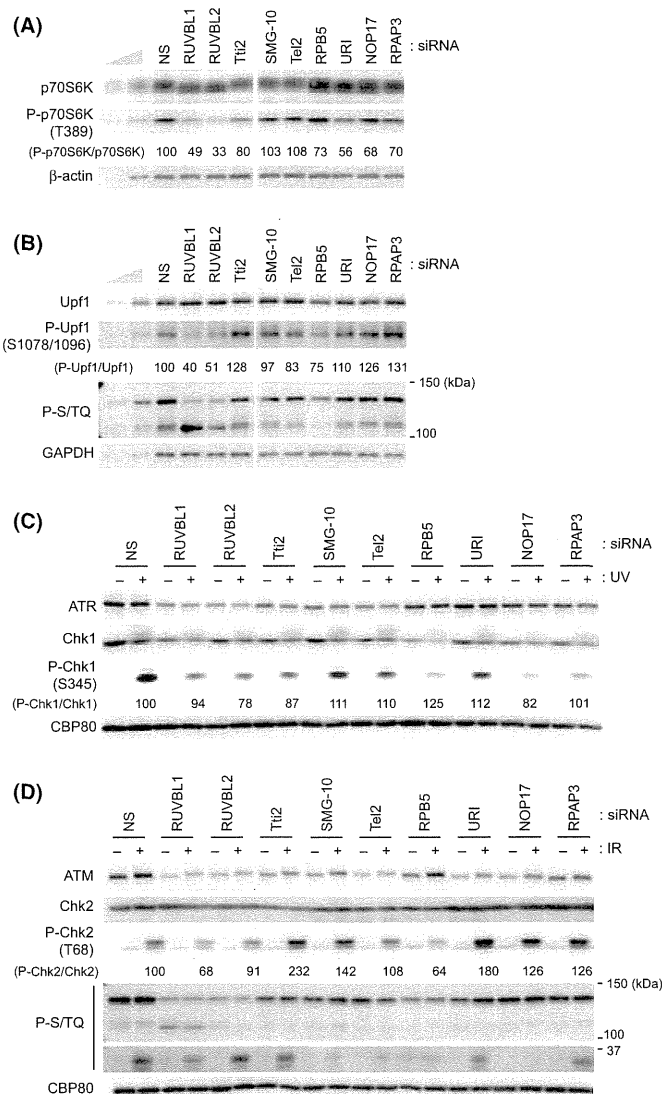


**Fig. 4.** Knockdown of RUVBL1/2 and Tel2 interacting proteins affects the phosphatidylinositol 3-kinase-related protein kinase (PIKK) signaling. (A,B) HeLa TetOff cells were transfected with the indicated siRNA. Sixty hours after transfection, total cell lysates were analyzed by western blotting with the indicated antibodies. Same knockdown samples were used in panels A,C,D in Figure 3, and panels A and B in Figure 4. To estimate protein abundances, 33 and 11% of the non-silencing (NS) control were loaded. (C,D) HeLa TetOff cells were transfected with the indicated siRNA. Sixty hours later, cells were untreated, treated with 100 J/m<sup>2</sup> of UV (C), or 10 Gy IR (D), and incubated for 1 h. Total cell lysates were analyzed by western blotting with the indicated antibodies. The anti-P-S/TQ antibody recognizes phosphorylated serine or threonine in the SQ motif, potential phosphorylation sites by ATM/ATR/SMG-1/DNA-PKcs (B,D). Relative phosphorylation levels of p70S6K (A), Upf1 (B), Chk-1 (C), Chk-2 (D) were indicated under each blot. ATM, ataxia telangiectasia mutated; ATR, ATM-and Rad3-related; DNA-PKcs, DNA-dependent protein kinase catalytic subunit; SMG-1, suppressor with morphological effect on genitalia 1.

VBL2 or Tel2 (Fig. 4B). Furthermore, strong reduction of the phosphorylation of a 110-kDa protein detected by the phospho-S/TQ antibody was observed by the knockdown of RPB5, but not others (Fig. 4B). In analogy to the situation with Hsp90 inhibition, Chk1 is downregulated by the knockdown of RUVBL1/2, Tel2 and their associated proteins (Figs 1D,4C). The relative level of ATR-mediated phosphorylation of Chk1 at Thr345 caused by UV irradiation was slightly decreased by the knockdown of RUVBL2, Tti2 and NOP17 (Fig. 4C). In contrast, knockdown of RUVBL1/2-associated and Tel2-associated proteins had different effects on the relative level of ATM-mediated phosphorylation of Chk2 at Thr68 in response to IR. Whereas knockdown of RUVBL1 or RPB5 decreased the Chk2 phosphorylation, knockdown of Tti2, SMG-10, URI, NOP17 or RPAP3 enhanced it (Fig. 4D). These results suggest that RUVBL1/2-associated or Tel2-associated proteins are involved in the PIKK signaling and that their degree of contribution differs according to each PIKK and its substrate. However, we cannot exclude the possibility that the different effect is resulting from knockdown efficiency of each molecule.

RUVBL2 and Hsp90 are substrates of S/TQ-directed protein kinases,<sup>(45)</sup> ATM, ATR, DNA-PKcs and SMG-1. This suggests possible mutual regulatory mechanisms among PIKK. We ana-

lyzed knockdown effects of each PIKK member on other PIKK protein abundance. As shown in Figure 5, knockdown of DNA-PKcs or mTOR caused downregulation of ATM.

## Discussion

In this study, we showed that Hsp90 regulates all PIKK members and PIKK-mediated signaling (Fig. 1). This finding highlights the importance of Hsp90 as a key regulator of signal transduction and a target of cancer therapy. ATM, ATR and DNA-PKcs are critical regulators of DNA damage response and repair,<sup>(46-48)</sup> and other PIKK members, SMG-1 and TRRAP, are also involved in these processes.<sup>(21-23)</sup> DNA repair pathway has been studied as a target for cancer therapy in combination with DNA-damaging drugs.<sup>(49)</sup> Moreover, NMD inhibition, including SMG-1 inactivation, has attracted attention as a novel anti-cancer strategy by induction of tumor immunity.<sup>(50,51)</sup> mTOR controls cell proliferation and angiogenesis, and mTOR inhibitors have been developed as antitumor agents.<sup>(52)</sup> Hsp90 is required for the maintenance of all PIKK and PIKK-mediated signaling, as we have shown here. Therefore, Hsp90 inhibition is expected to yield additive effects of all PIKK disruption-mediated defect of cellular function mentioned above. Thus, our results support

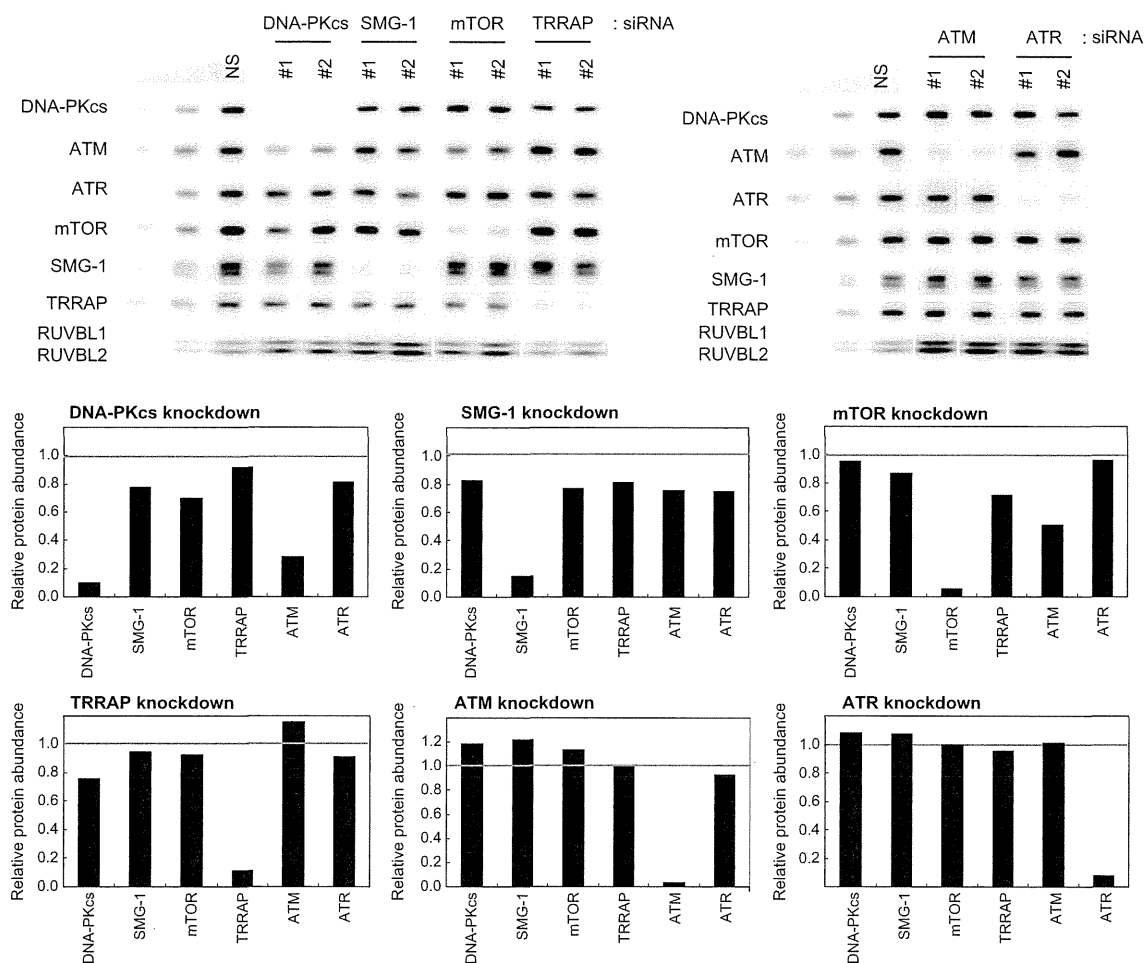


**Fig. 5.** Knockdown of DNA-PKcs or mTOR reduces the ATM abundance. HeLa TetOff cells were transfected with two independent siRNA targeted to each phosphatidylinositol 3-kinase-related protein kinase (PIKK). Sixty hours after the transfections, total cell lysates were analyzed by western blotting with the indicated antibodies. To estimate the PIKK abundance, 33 and 11% of the nonsilencing (NS) control sample were loaded. The relative protein levels of each PIKK compared with the NS control levels were graphed. The values are an average of the data from two siRNA from two independent experiments. ATM, ataxia telangiectasia mutated; ATR, ATM-and Rad3-related; DNA-PKcs, DNA-dependent protein kinase catalytic subunit; mTOR, mammalian target of rapamycin; SMG-1, suppressor with morphological effect on genitalia 1; TRRAP, transformation/transcription domain-associated protein.